AN EXPERIMENTAL STUDY ON CO_2 AND BUTANE ADSORPTION ON ACTIVATED CARBON

By

Görkem Oğur

B.S., Chemical Engineering, Boğaziçi University, 2007

Submitted to the Institute for Graduate Studies in
Science and Engineering in partial fulfillment
of the requirements for the degree of
Master of Science

Graduate Program in Chemical Engineering

Boğaziçi University

2009

to my family and friends

ACKNOWLEDGEMENTS

First of all, I would like to express my sincere gratitude to my thesis advisor Prof. Dr. A. Erhan Aksoylu. He constantly motivated and guided me with his innovative vision. His trust in me and my study methods gave me confidence throughout this period.

I am also very grateful to Assoc. Prof. Hasan Bedir and Assist. Prof. A. Kerim Avcı for their support and sparing their valuable time for reading and commenting on my thesis.

Şeyma Özkara Aydınoğlu, Burcu Selen Çağlayan, Feyza Gökaliler, Ilgaz Soykal and Sadi Tandal Tezcanlı deserve special thanks as my mentors. Their invaluable experience and will to help has made this study possible.

Heartful thanks to Eralp Bolkent, Sabriye Güven, İlker Öztürk, Murat Şen, Can Yaman and other members of Gençlerbirliği, who filled my last two years with joyful moments and laughter. Feeling their friendship and support was an invaluable gift for me.

I also would like to thank to Tuğba Davran Candan, Elif Ercan, Aslıhan Sümer, and Sevinç Tuna who made the laboratory a friendly environment.

I owe a deep thanks to skillful technicians Bilgi Dedeoğlu and Nurettin Bektaş, for assisting me many times with their superior technical experience.

Cordial thanks to supporting personnel Fatma Coşkun, Melike Gürbüz, Kamuran Taylan and Yakup Bal for their support.

This work is partially supported by Ford Otosan A. Ş. through a joint project ÜG29. The financial support provided by State Planning Organization through project DPT 07K120630 is also acknowledged.

ABSTRACT

AN EXPERIMENTAL STUDY ON CO_2 AND BUTANE ADSORPTION ON ACTIVATED CARBON

The aim of this study is to investigate the effect of textural and surface chemical properties of activated carbon (AC) samples on their CO_2 and butane adsorption capacities and adsorption behavior. In the first part of the study, the effects of surface chemistry, oxidation method, Na_2CO_3 impregnation and calcination temperature on selective CO_2 adsorption behavior of activated carbon samples, which had been previously prepared by B. S. Çağlayan, was determined under dynamic conditions. Adsorption experiments were performed with a gravimetric analyzer and gas concentrations were analyzed with a mass spectrometer. Oxygen bearing surface groups of unimpregnated samples were determined via Temperature Programmed Surface Group Decomposition (TPSGD or TPD) deconvolutions. The results revealed that air oxidation increased the amounts of anhydrides and carbonyl/quinones whereas reduced the amounts of lactones and carboxyls. Total surface area and CO_2 adsorption capacity increased with air oxidation. HNO_3 oxidation had a strong influence on surface groups. Increase in the acidic carboxylic sites and reduction in the BET surface area upon HNO_3 treatment, resulted in a decrease in the CO_2 adsorption capacity. However, the results revealed that HNO_3 oxidization has enhanced Na_2CO_3 dispersion more than air oxidation. This enhancement was attributed to increase in the carboxylic surface groups as well. It was discovered that Na_2CO_3 impregnation enhanced both reversible and irreversible CO_2 adsorption. Calcination temperature, on the other hand, had no effect on the CO_2 adsorption behavior up to 250 °C, however, sample calcined at 300 °C showed more superior adsorption capacity in comparison with other calcined samples. All samples showed selective CO_2 adsorption behavior whereas Na_2CO_3 impregnated samples irreversibly adsorbed H_2 and CO to a certain extent as the gases came into contact with the adsorbent.

In the second part of the study, the relation between AC characteristics of commercial activated carbons (AC10, AC11 and AC12), which were provided by Ford Otosan A. Ş., and their butane adsorption capacity and characteristics were studied. For this purpose, butane adsorption isotherms were obtained at 40 °C, 70 °C and 100 °C by using a gravimetric analyzer in static mode. Oxygen bearing surface groups and total surface areas of the samples were determined via TPSGD/TPD and BET methods, respectively. Butane adsorption capacity of samples AC10, AC11 and AC12 was determined as 28.29%, 29.56% and 49.67% by weight at 1 bar and 40 °C respectively. Results revealed that there is a strong relationship between surface area and adsorption capacity. In addition, it was found out that lactone, phenol and carbonyl/quinone groups has no significant contribution on the adsorption capacity whereas, carboxyl and anhydride surface groups may have a limited positive contribution on the adsorption capacity. High correlation was obtained upon fitting Langmuir isotherm on the adsorption data showing butane adsorption on AC samples can be represented with Langmuir isotherm. The heat of adsorption was calculated as -13.2 kj/mol, -12.6 kj/mol and -16.5 kj/mol for samples AC10, AC11 and AC12 respectively from modified form of Clasius Clapeyron equation by using Langmuir constants obtained.

ÖZET

AKTİF KARBON ÜZERİNE CO_2 VE BÜTAN ADSORPSİYONU ÜZERİNE DENEYSEL BİR ÇALIŞMA

Mevcut çalışmanın amacı, aktif karbon (AK) numunelerinin, yapısal ve yüzey kimyası özelliklerinin, AK örneklerinin CO_2 ve bütan adsorpsiyon kapasitesi ve davranışına olan etkisinin incelenmesidir. Çalışmanın birinci bölümünde, daha önce B. S. Çağlayan tarafından hazırlanmış numunelerin, seçici CO_2 adsorpsiyon davranışı üzerinde, oksidasyon metotları ve yüzey kimyasının, Na_2CO_3 emdirilmesinin ve kalsinasyon sıcaklığının etkileri belirlenmiştir. Adsorpsiyon deneyleri, ağırlık ölçümüne dayalı analizör ile yapılmış ve gaz kompozisyonu kütle spektrometresi cihazıyla analiz edilmiştir. Emdirilmemiş numunelerin oksijen tutan yüzey gurupları sıcaklık programlamasıyla salınım (SPS) metoduyla belirlenmiştir. Sonuçlar; hava oksidasyonun, anhidrit ve karboni/kuinon miktarını arttırdığı fakat lakton ve karboksil miktarını azalttığını ortaya çıkarmıştır. Toplam yüzey alanı ve CO_2 adsorpsiyon kapasitesi hava oksidasyonuyla yükselmiştir. HNO_3 oksidasyonunun yüzey grupları üzerinde güçlü bir etkisi vardır. HNO_3 uygulamasıyla karboksilik bölgelerin artması ve BET yüzey alanının düşmesi, CO_2 adsorpsiyon kapasitesinde düşmeye sebep olmuştur. Fakat sonuçlar HNO_3 uygulamasının, Na_2CO_3'ün yüzeyde yayılmasını, hava oksidasyonundan daha fazla arttırdığını ortaya çıkarmıştır. Bu artış da karboksilik yüzey gruplarının artışına bağlanmıştır. Na_2CO_3 emdirilmesinin, hem tersinir hem de tersinmez CO_2 adsorpsiyonunu arttırdığı ortaya çıkmıştır. Öte yandan, 250 °C ye kadar, kalsinasyon sıcaklığının adsorpsiyon gidişatına etkisi olmamıştır, fakat 300 °C'de kalsine edilmiş numune, diğer kalsine edilmiş numunelere göre, daha üstün adsorpsiyon kapasitesi göstermiştir. Tüm numuneler seçici adsorpsiyon davranışı göstermiş; buna karşın Na_2CO_3 emdirilmiş numuneler ilk temasta belli bir ölçüde H_2 ve CO'yu tersinmez şekilde adsorbe etmiştir.

Çalışmanın ikinci bölümünde, Ford Otosan A. Ş. Tarafından temin edilen ticari aktif karbon numunelerinin (AC10, AC11 ve AC12), fiziksel ve kimyasal yüzey özellikleriyle

adsorpsiyon kapasiteleri ve adsorpsiyon davranışları arasındaki ilişki araştırılmıştır. Ağırlık ölçümüne dayalı analizör ile 40 °C, 70 °C ve 100 °C'de, durgun şartlarda, sabit sıcaklık eğrileri elde edilmiştir. Numunelerin oksijen tutan yüzey grupları ve toplam yüzey alanı, sırasıyla BET ve SPS ile belirlenmiştir. AC10, AC11 ve AC12 numunelerinin bütan adsorpsiyon kapasiteleri 1 bar ve 40 °C'de sırasıyla, ağırlıkça %28.29, %29.56 ve %49.67 olarak belirlenmiştir. Sonuçlar yüzey alanıyla adsorpsiyon kapasitesi arasında güçlü bir bağlantı olduğunu ortaya çıkarmıştır. Bununla birlikte, adsorpsiyon kapasitesinde; lakton, fenol ve karbonil/kuinon gruplarının önemli bir etkileri olmadığı, fakat karboksil ve anhidrit yüzey gruplarının sınırlı bir şekilde olumlu etkileri olabileceği görülmüştür. Langmuir sabit sıcaklık eğrisi adsorpsiyon verilerine oturtulduğunda yüksek korelasyon elde edilmesi, bütan adsopsiyonunun Langmuir sabit sıcaklık eğrisi ile temsil edilebileceğini göstermiştir. Elde edilen Langmuir sabitleriyle, Clasius Clapeyron denkleminin modifiye hali kullanılarak, AC10, AC11 ve AC12 numunelerinin adsorpsiyon enerjisi, sırasıyla -13.2 kj/mol, -12.6 kj/mol ve -16.5 kj/mol olarak hesaplanmıştır.

TABLE OF CONTENTS

LIST OF FIGURES

LIST OF TABLES

LIST OF SYMBOLS/ABBREVIATIONS

A_c	Clasius Clapeyron constant containing the entropy term
A_{CO2}	Weight per cent adsorbed CO_2 in the first cycle
A^2_{CO2}	Weight per cent adsorbed CO_2 in the second cycle
A_{H2+CO}	Weight per cent adsorbed H_2 and CO
b	Langmuir constant
D^1_{CO2}	Weight per cent desorbed CO_2 in the first cycle
D^2_{CO2}	Weight per cent desorbed CO_2 in the second cycle
K	Constant characterizing pore size distribution in D-R equation
W	Micropore volume in D-R equation
W_0	Initial weight
W_1	Weight after H_2 and CO adsorption
W_2	Weight after adsorption of CO_2 in first cycle
W_3	Weight after desorption of CO_2 in first cycle
W_4	Weight after adsorption of CO_2 in second cycle
W_5	Weight after desorption of CO_2 in second cycle
Vm	Langmuir constant
β	Affinity constant
AC	Activated carbon
BET	Brunauer-Emmet-Teller
BOS	Birleşik Oksijen Sanayi
CMS	Carbon molecular sSieve
DSMS	Dynamic sampling mass spectrometer
DR	Dubinin- Radushkevitch
IGA	Intelligent gravimetric analyzer
MFC	Mass flow controller
PROX	Preferential CO oxidation
TPD	Temperature programmed decompositions/desorption

TPSGD	Temperature programmed surface group determination
WGS	Water gas shift
VCM	Vinyl chloride monomer

1. INTRODUCTION

Global warming is a serious threat to the environment; as its consequences getting detrimental, the regulations about gas emissions become more and more stringent. Thus, developing alternative energy production methods has become a major research area. Hydrogen Fuel Cell is considered as a green energy source for both mobile transport and electricity production. Proton exchange membrane (PEM) fuel cells are preferable in many areas due to their low temperature application and mobility. Producing H_2 rich stream from natural gas by steam reforming is considered as a cost effective method since there are still rich natural gas reservoirs and distribution of natural gas is well established.

Major drawback of producing H_2 from CH_4 (or from other hydrocarbons) in order to use in PEM fuel cells is that PEM is very sensitive to CO content; even 15 ppm CO in the stream can poison the membrane. Applying water gas shift (WGS) reactions to reduce CO content and to enrich H_2 in the stream and applying preferential CO oxidation (PROX) after WGS reactions to further convert CO to CO_2 is well established in the literature.

Eliminating CO_2 with adsorption at the WGS exit is advantageous in 3 ways: (i) Adsorption reduces the emission of CO_2 which is a greenhouse gas. (ii) It has been reported that CO_2 can undergo reverse water gas shift reaction to form CO and H_2O thus removal of CO_2 eliminates a potential threat (Bruijn *et al*. 2002). (iii) Reduction in product concentration of PROX reaction will increase its yield by Le Chatelier principle.

High surface area, cheap manufacturing costs and variable surface chemistry make activated carbons a good candidate as an adsorbent. Majlan *et al*. (2009) has already applied activated carbon adsorbents to purify H_2 at the water gas shift exit and managed to reduce CO_2 concentration from %5 to 7.0 ppm and CO from 4000 ppm to 1.4 ppm in a gas mixture of $H_2/CO_2/CO$.

Textural characteristics (surface area, microporosity etc.) and surface chemistry (oxygen, nitrogen functionalities) are the major categories that affect the adsorption

capacity and characteristics. The effect of surface area on adsorption is well established whereas correlation between the amount of oxygen bearing surface groups and adsorption behavior is still unclear. Surface area is measured commonly by N_2 adsorption at 77 K (BET method) and the amount and type of oxygen bearing surface groups can be determined by using temperature programmed surface group decomposition (TPSGD / TPD).

There are several treatments that can change the textural and properties and surface chemistry of AC. It has been reported that air oxidation and HNO_3 treatments have positive effects on dispersion of metal atoms when AC is to be used as a catalyst support (Aksoylu *et al.*, 2000).

One of the purposes in this study is to determine the selective CO_2 adsorption capacity and characteristics of AC and Na_2CO_3 impregnated ACs from a mixture that contains 50 % H_2, 15 % CO_2, 2 % CO and balance He.

Surface chemistry determination via TPD, surface area determination via BET and selective CO_2 adsorption experiments were carried out on samples: Norit ROX (AC0), HCl washed Norit ROX (AC1), air oxidized Norit ROX (AC2), HNO_3 oxidized Norit ROX (AC3). In addition, selective CO_2 adsorption behaviors of Na_2CO_3 impregnated air oxidized and calcined Norit ROX (AC4a, AC4b, AC4c) and Na_2CO3 impregnated HNO_3 oxidized and calcined Norit ROX (AC5a, AC5b, AC5c) were investigated. Effect of surface area and surface chemistry on selective CO_2 adsorption as well as effect of oxidation method, Na_2CO_3 impregnation and calcination temperature were discussed.

The highest source of hydrocarbon emissions on road transport are considered as the evaporation loses from gas tanks of vehicles (Mellios and Samaras, 2007). AC loaded canisters are used at the purge exit of the fuel tanks as a filter in order to prevent hydrocarbon emission to the environment. Another purpose of the current study is to determine the adsorption capacity and behavior of commercial activated carbons used in canisters. The adsorption capacity for butane, which represents the vapor in the fuel tank were determined for three commercial AC samples (AC10, AC11, AC12), which are readily used in the commercial carbon canisters and supplied by Ford Otosan A. Ş.

Adsorption isotherms at 40 °C 70 °C and 100 °C were obtained for all samples and heats of adsorption were calculated via utilizing Langmuir parameters, which are found upon fitting the obtained adsorption data to Langmuir adsorption isotherm equation.

Oxygen bearing surface groups were determined by TPSGD and surface areas were obtained with BET method. The link between butane adsorption capacity and surface chemistry/surface area were discussed.

Chapter 2 of this study contains general information about adsorption, adsorption isotherms and activated carbon adsorption as well as the information on relevant previous studies. In Chapter 3, experimental setups and procedures will be given in detail. In Chapter 4, results of the adsorption experiments and the possible correlations between AC characters and adsorption behavior will be discussed. In chapter 5 conclusions that are reached in the discussion of the study are stated.

2. LITERATURE SURVEY

2.1. Activated Carbons

Owing to their high surface area and modifiable surface chemistry; Activated Carbon is a highly desired material in the industry as adsorbent, catalyst and catalyst support. Availability of raw material and cheap manufacturing cost makes ACs more and more attractive. There is an abundance of study in the literature concerning AC properties and applications.

Though activated carbon materials are mainly manufactured from wood, coal, lignite, coconut shell and peat, they can be produced from various materials ranging from fruit pits to used tires (Allen *et al.*, 1999). ACs are produced from suitable precursors in two ways: chemical and physical activation. Precursor materials, having immature pore structure, are burn off and gasified in order to have disordered pore network having oxygen bearing surface groups. In chemical activation carbonization and activation steps are performed simultaneously at 600-800°C by using H_3PO_4 and $ZnCl_2$ as activating agents. In physical activation however, carbonaceous precursor is thermally decomposed first in an air free environment at 600-800°C, during which, most of the non carbon elements such as hydrogen oxygen and nitrogen are withdrawn, leaving a carbon based porous structure. Following the carbonization step, precursors are activated with steam or CO_2 at 800-1100°C, which extends the pore structure network leading to a very high surface area product. AC, can be washed with pure water or mineral acids to remove the ash content following the activation step In order to diminish potential catalyst poisons, an additional washing step is highly desired if the activated carbon is to be used as catalyst support (Auer E., 1998).

Due to its microporous characteristics AC has high surface area and is widely used as adsorbent and catalyst support.

2.1.1. Activated Carbon as Adsorbent

Adsorption is the physical bonding of adsorbate molecules onto the surface of the adsorbent led by the unbalanced molecular forces of the adsorbent surface. There are two kinds of adsorption namely: physical adsorption and chemical adsorption. Physical adsorption is analogues to condensation as the adsorbed molecules bonds to surface and on top of each other by weak Van der Waals forces leading to multilayer adsorption. In chemical adsorption on the other hand, adsorbate molecules interacts only with surface of the adsorbent and form stronger chemical bonds, which involve sharing of electrons. In chemical adsorption, the interaction is only with the surface of the adsorbent which results in a monolayer adsorption. Energy of adsorption clearly reflects the difference between the two kinds of adsorption; ΔH adsorption for physical adsorption is in the range of energy of condensation (10-20kj/mol) whereas ΔH of adsorption is much greater for chemical adsorption; which has values in the range of 40 – 400kj/mol. As will be discussed in detail in the text; Brunauer-Emmett-Teller (BET), and Dubinin equations represents the isotherm data of physical adsorption, whereas Langmuir and Freundlich equations are in good correlation with the both physical and chemical adsorption on porous carbons (Bansal and Goyal, 2005).

There are many parameters affect the adsorption phenomena, such as nature of the adsorbent and adsorbate, the surface chemistry and surface area of the adsorbent, temperature and pressure of the system. It is well known that increasing surface area and porosity increases the adsorption capacity of the adsorbents. Both the textural properties, such as high surface area and micro pore network, and the surface chemistry (ie. The types and abundance of oxygen bearing surface groups) make the ACs as one of the most widely used adsorbents. AC adsorbents are usually used in the removal of hazardous components from waste gases and liquids (Bansal and Goyal, 2005).

2.1.2. Aqueous Phase Adsorption with Activated Carbon

Early production of ACs is over 500,000 tons. Nearly 80% of all the AC adsorbents are used in the removal of pollutants from the aqueous phase (Moreno-Castilla and Rivera-Utrilla, 2001). With respect to the type of aqueous application, AC treatment can be

divided into three categories. Treatment of the drinking water or municipal water is the first category. It involves large scale treatment of water from rivers or lakes before dispersing. Treatments are necessary for removal of hazardous species and to increase the water quality in terms of odor and taste. The second category is the treatment of water before utilizing it in the industrial applications, such as water for the cooling towers or heat exchangers. The last category is the adsorption of the toxic and harmful species from the waste water before disposing it to environment (Bansal and Goyal, 2005).

Depending on the surface character of the carbon material and ph of the aqueous media, an electric charge is generated when the activated carbon contacts with the aqueous solution. This electrical charge is formed whether due to the dissociation of the surface functional groups of the AC or the adsorption of the ions from the aqueous media (Quinlivan and Knappe, 2002).

Adsorption capacity and characteristics of activated carbons are widely studied and reviewed for aqueous removal of inorganic pollutants such as copper, chromium, mercury, cadmium, cobalt, nickel, zinc, arsenic as well as for removal of organic pollutants such as: halogenated organic components, natural organic components, phenolic compounds, nitro and amino compounds, pesticides, dyes, drugs and toxins (Dias *et al.*, 2007; Bansal and Goyal, 2005).

2.1.3. Activated Carbons as Gas Adsorbents

Gas phase applications of Activated Carbons are very large in number. Some application of AC according to Marsh and Rodriguez-Reinoso (2006) are listed below:

- Personal protection.
- Cigarette filters.
- Industrial gas masks. Chemical warfare agent protection, including clothing, gas masks, and atmospheres in warships, submarines, tanks and aircraft.
- Effluent gas purification.
- Industrial off-gas purification, removal of SO_2, H_2S, CS_2, etc.

- Petroleum refineries.
- Sewage and geothermal plants.
- Vinyl chloride monomer (VCM) plants and solvent recovery in general.
- Separation of gas mixtures using carbon molecular sieves (CMS).
- Organic and inorganic process catalysis, both as a support material and as a catalyst.
- Adsorption of radionuclides.
- Natural gas storage and purification.
- Automobile/gasoline recovery.
- Odor control generally.

Among listed, automobile\gasoline recovery and gas purification are special interests of this text and these topics will be discussed in detail later.

From the environmentalist point of view, one of the most important applications of AC is removal of hazardous components from waste gases. Increase in the industrial waste gases began to threat environment, thus the regulations about the stack gas streams are becoming more and more stringent. The level of hazardous materials in the environment and the current regulations resulted in the need of advance filtering systems for various gas emissions. Removal of pollutants from flue gas plays a significant role in the emission reduction. Major air pollutants in the flue gases are SO_2, CO, NO_x and mercury.

Combustion of fossil fuels is the main reason of the increasing SO_2 concentration in air. It is well known that emitted SO_2 in the atmosphere is one of the strongest precursors initiated the acid rain. A common way to remove SO_2 from stack gases are dry removal of SO_2 by using activated carbon. The strongest reasons for ACs to be chosen as the adsorbents for these processes are high adsorption characteristics and easy manufacturing from cheap materials and wastes such as palm shell and used tires (Sumathi *et. al.*, 2009; Karatepe *et al.*, 2008).

Mercury emissions from flue gases are also a big concern due to its adverse effect on the living. Activated carbons offers a great potential for removing mercury vapor which

can not be removed effectively using current air pollution control devices. Various researches are conducted investigating the effect of textural properties and impregnation techniques of activated carbon materials and the effect of the adsorption conditions on the adsorption ability of activated carbons used in the removal of mercury vapor effectively from flue gas streams (Yang *et. al.*, 2007; Yan *et al.*, 2005).

In addition of removing hazardous components, utilization of AC in purification of gas streams has been reported by researchers (Chlendi and Tondeur, 1995; Majlan *et al*., 2009) and purification of hydrogen from an H_2 rich gas stream is of special interest of the current study and will be discussed in detail in section 2.3.

2.1.4. Activated Carbons as Catalyst and Catalyst Support

Activated carbons are used in many reactions as catalysts or catalyst supports or both. High surface area and different kinds of surface functional groups are considered as the main reasons for the high activity of the AC surface, however, the relationship between the surface groups and reaction mechanism are still unclear (Xue *et al.*, 2008).

One of the application areas of activated carbon catalysts is the catalytic reduction and oxidation of NO. NO_x are considered as hazardous agents which can deplete ozone layer. Since NO_2 can easily be removed by water, oxidation of NO to NO_2 is a way of elimination NO in the flue gas stream. It is stated that activated carbons are promising catalyst in dry oxidation of NO. Although catalytic activity is reduced in the humid environment, heat treatment over 600°C enhances the H_2O resistance via decomposing some of the oxygen bearing surface groups (Isao Mochida). In contrast, when AC is used as the catalyst support for CuO, increase in the surface oxygen groups favors the CuO dispersion on AC leading to an increase in the NO reduction ability of CuO/AC (Xue *et al.*, 2008).

H_2 production by methane pyrolisis and decomposition, ozonation of p-chlorobenzoic acid, oxidation of H_2S and SO_2, formic acid decomposition, dehydrogenation of isopropyl alchocol, synthesis of carbonyl chloride ($COCL_2$) can be given as other examples of AC catalyzed reactions (Rodriguez-Reinoso, 1998).

Although ACs are promising catalysts, they are more often used as catalyst supports in the industry due to the fact that they have all the requirements necessary to be used as support such as high temperature stability, porosity and high surface area. In addition, they are resistant in both acidic and basic media. Most common active metals supported on AC are platinum, palladium, nickel and iron. ACs have higher porosity and surface area than alumina and silica but the porosity is mostly in the size of micropores. Although studies show that microporosity favors dispersion of metal atoms to a certain extent, it can be a drawback when large molecules, such as large active metal groups, reactants or products, are introduced to the system. It is also seen in literature that not only the porosity but also the nature of the surface chemistry and its interactions with the precursor solutions has an effect on dispersion and\or activity of metal atoms (Aksoylu *et al.*, 2001; Rodriguez-Reinoso, 1998).

2.2. Activated Carbon Characterization

Activated Carbons are among the group of non-graphitizable porous carbons. Surface area of ACs can be up to 3500m^2/g (Saha *et al.*, 2008). Although high sorption capacity is the result of high surface area to a large extent, recent studies has confirmed that surface chemistry also plays a significant role in adsorption capacity. Thus, both textural and surface chemistry characterizations are necessary for complete characterization of AC adsorbents.

2.2.1. Textural Properties and Characterization

As illustrated in Figure 2.1, porous network of AC are constituted by crumpled imperfect sections of graphitic lamellae which are bonded together to form a three-dimensional network. Variations in this network affect not only the porosity but also the physical characteristics such as bulk density and hardness. Porosity of ACs is usually classified in three categories. Pores having width less than 2nm are called micropores which contribute most to the high surface area and adsorption capacity. Pores having width between 2-50 nm are called mesopores. Mesopores are important in adsorption of large molecules. Last category is macropores having width larger than 50nm. Transportation of molecules into the interior surface and micropores occurs through the macropores and

mesopores of the AC (Rodriguez-Reinoso and Molina-Sabio, 1998). Sometimes an additional category is used in the literature to refer pores having width less than 0.6-0.7nm which are named as narrow micropores (Reinoso *et al*., 1989; IUPAC, 1972).

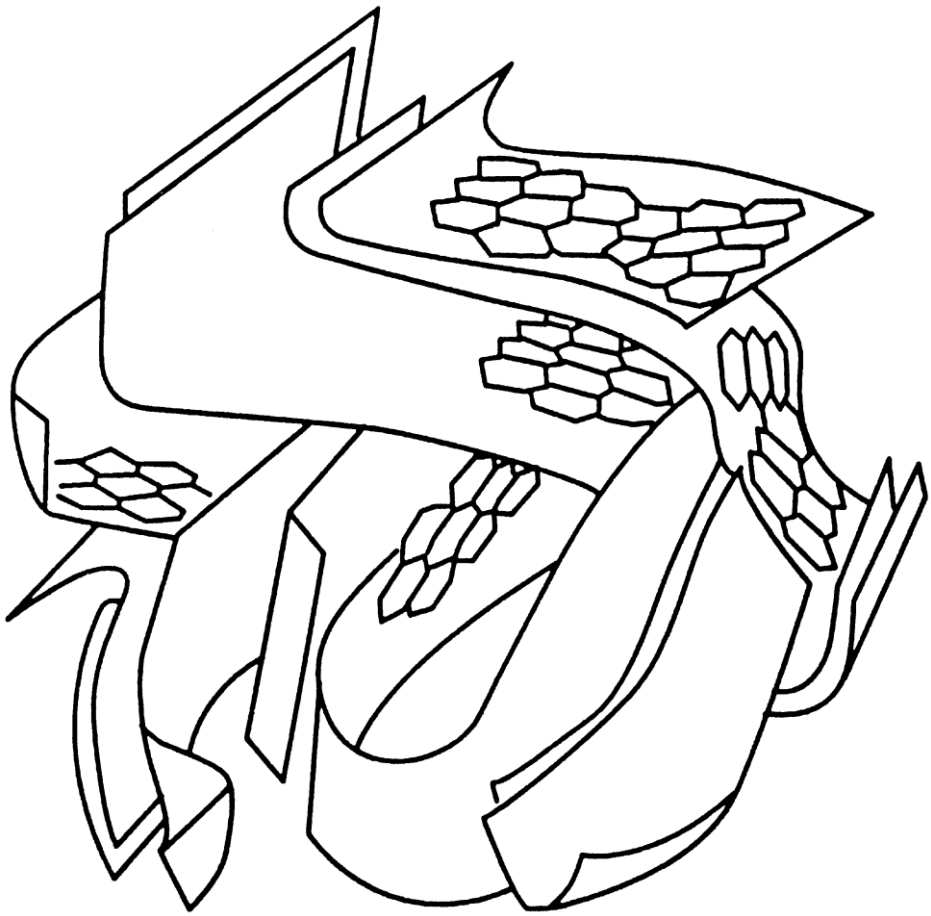

Figure 2.1 Schematic representation of the structure of activated carbon (Rodriguez-Reinoso and Molina-Sabio, 1998).

Gas adsorption studies are the most applied methods to investigate textural properties of porous materials. It is possible to determine surface area of the adsorbent, the volume of the pores, and their size distribution, the heat of adsorption, and the relative absorbability of a gas or a vapor on a given adsorbent can be found through using the equilibrium adsorption isotherms. There are five main types of isotherm equations as illustrated in Figure 2.2 (Bansal and Goyal, 2005).

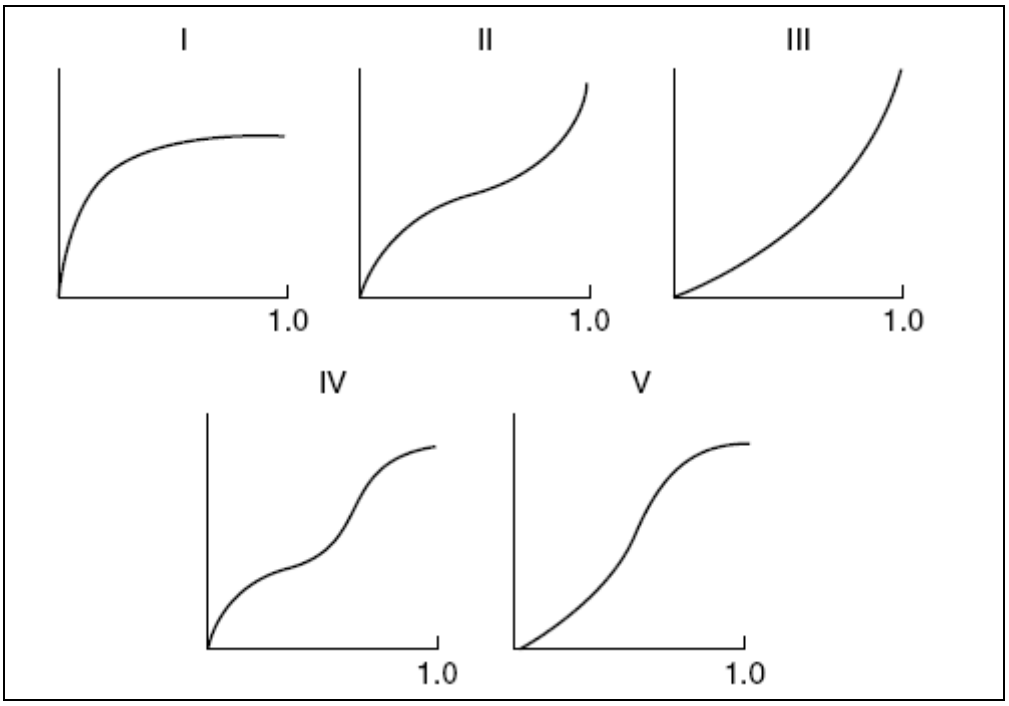

Figure 2.2 Five main types of adsorption isotherms (Bansal and Goyal, 2005)

On the basis of those different adsorption behaviors, there are several isotherm equations derived to represent isotherm data. Langmuir, Brauner-Emmet-Teller, Dubinin-Radushkevitch, Freundlich and Temkin are considered as the most important equations.

2.2.2.1. Langmuir Isotherm Equation. Langmuir equation is the first absorption isotherm which is theoretically developed. Many other equations are either inspired from the Langmuir concept or based on this equation. Langmuir equations are of type I and based on the following theoretical assumptions:

- The adsorbed entities (atoms or molecules or ions) are attached to the surface at definite localized sites.
- Each site accommodates one and only one adsorbed entity.
- The energy state of each adsorbed entity is the same at all sites on the surface independent of the presence or absence of other absorbed entities at neighboring sites. (Langmuir, 1918)

Theory of this equation is based on that the rate of adsorption is equal to the rate of desorption and the number of unoccupied sites for adsorption can be found by subtracting

occupied sites from total number of sites. After derivation, linearized form of the equation is given as (Langmuir, 1918):

$$\frac{P}{V} = \frac{1}{bVm} + \frac{P}{Vm} \tag{2.1}$$

where P is the partial pressure, V is the volume adsorbed, Vm is the monolayer volume of the adsorbed gas and b is a constant related to the adsorption system. By using a plot of P/V vs. P, monolayer coverage and constant b can be calculated.

Specific surface area can be obtained by using the following relationship:

$$S_t = \frac{NA_g V_m}{V} \tag{2.2}$$

where N is the Avogadro number ($6.02.10^{23}$ molecules/gmole), V is the molecular volume of the adsorbed gas at reference conditions and A_g is the cross sectional area of each adsorbed molecule.

2.2.1.2. Brunauer-Emmet Teller (BET) Isotherm Equation. BET isotherm is the most widely used method in textural characterization of porous media to determine surface area and total pore volume from physisorption data. It takes both the monolayer and the multilayer adsorption behavior of gases into account. It is mostly applicable to type II isotherm in which, after certain extent, gas molecules condenses on top of each other forming multilayer adsorption with increasing partial pressure.

BET theory, in its original form, is an extension of Langmuir theory to multilayer adsorption. Theory is based on the same principle; in equilibrium, the rate of adsorption in each layer is equal to the rate of evaporation from that layer. It was assumed that the molecules in the first layer are located on a set of equivalent surface sites and that these molecules are forming sites for the second layer. In the derivation of BET equation, no lateral adsorbate-adsorbate interactions are taken into account. The following assumptions are necessary to simplify the BET model further;

- In all layers after the first, the adsorption-desorption conditions are identical.
- In all layers except the first, the energy of adsorption is equal to the condensation.
- At saturation pressure ($P = P_0$) the multilayer has infinite thickness (Gürdağ, 2001).

With the help of these assumptions Brunauer, Emmet, Teller (1938) has formed their first and most useful form of equation,

$$\frac{P}{V(P_0 - P)} = \frac{1}{cV_m} + \left[\frac{c-1}{cV_m}\right]\frac{P}{P_0} \tag{2.3}$$

where V is the volume adsorbed (cm^3), P is the partial pressure (mmHg), P_0 is the saturation pressure or vapor pressure of the adsorbate at system temperature (mmHg). To calculate Vm, monolayer coverage (cm^3), and c which is a constant for temperature and the nature of the gas solid system using the straight line plot, $\frac{P}{V(P_0 - P)}$ against P/P_0 is convenient. Specific surface area then can be found by using equation 2.2.

2.2.1.3. Dubinin- Radushkevitch (D-R) Isotherm Equation. Although D-R equation was originally proposed as an empirical relationship, it became the fundamental relationship to describe adsorption phenomena in microporous sorbents quantatively. It is based on the assumption that the mechanism of adsorption in micropores was pore filling rather than layer by layer surface coverage. Equation is very useful for the systems having only Wan der Waals forces that dominantly determine the adsorption behavior, such as the micropores of AC. On that basis, D-R equation is widely used to describe the high surface area AC materials (Hutson and Yang, 1997).

Dubinin and Radushkevich suggested that for activated carbons, the distribution of micropores based on their volumes can be represented as Gaussian functions and following equation is obtained upon simplification:

$$\ln W = \ln W_0 - D\left(\ln \frac{P_0}{P}\right)^2 \tag{2.4}$$

$$D = \frac{K}{\beta^2}(RT)^2 \tag{2.5}$$

where W_0 is the micropore volume, K is a constant characterizing pore size distribution and β is the affinity constant that is independent from temperature and nature of the adsorbent porosity. It is also referred as the absorbability of a vapor with respect to the standard vapor, in most cases benzene. β values can be found for various gases in the literature (Dubinin and Timofeev, 1946; Bansal and Goyal, 2005).

As depicted in equation 2.4, plotting $\ln W$ vs. $(\ln P_0/P)^2$ should give a straight line and from slope and intercept, constant K and micropore volume W_0 can be calculated. It is stated that in the relative pressure range of 10^{-5} to 0.2, the equation is valid for various adsorbates, such as nitrogen benzene and hydrocarbons, on activated carbons (Bansal and Goyal, 2005).

It is widely accepted that DR equation can be applied to the type I isotherm behavior in low relative pressures since it is suggested that this behavior is a result of micropore filling on the other hand the slope of the plateau occurring in high relative pressures is due to the multilayer adsorption in mesopores, macropores and on the external surface. Additionally there are some variations of D-R equation called α and t plots. These plots are methods for estimation of micropore volumes by comparing the isotherm to an isotherm of a non microporous reference material, preferably the same one. Reinoso (1986) and his co-workers have devised α plots with activated carbons whose micropore volume were reduced with heat treatment at 2047 K and these plots were used as reference plots in the literature by the leading activated carbon researchers working on textural characterization of activated carbons (Pereira *et al.*, 2004).

It is widely accepted that by applying D-R equation to N_2 isotherm data at 77K, the micropore volume (width <2nm), and similarly, applying D-R equation to CO_2 isotherm

data at 273 K, the total volume of narrow micropores (width <0.6-0.7nm) can be estimated (Silvestre-Albero *et al*., 2009).

2.2.2. Surface Chemistry of Activated Carbon

Prior to the discussion on the surface structure, it is crucial to give information on the inner crystalline structure of AC. During carbonization step, elimination of non carbon elements such as oxygen, nitrogen and hydrogen leaves carbon atoms in aromatic sheets. These sheets (as illustrated in Figure 2.1), forms crystalline structures of AC, which differs from the structure of graphite in terms of interlayer spacing and orientation. As seen from Figure 2.2, AC crystalline structure has defects and is less ordered than that of graphite. These defects consist of heteroatoms such as oxygen and nitrogen as well as vacancies (Bansal and Goyal, 2005).

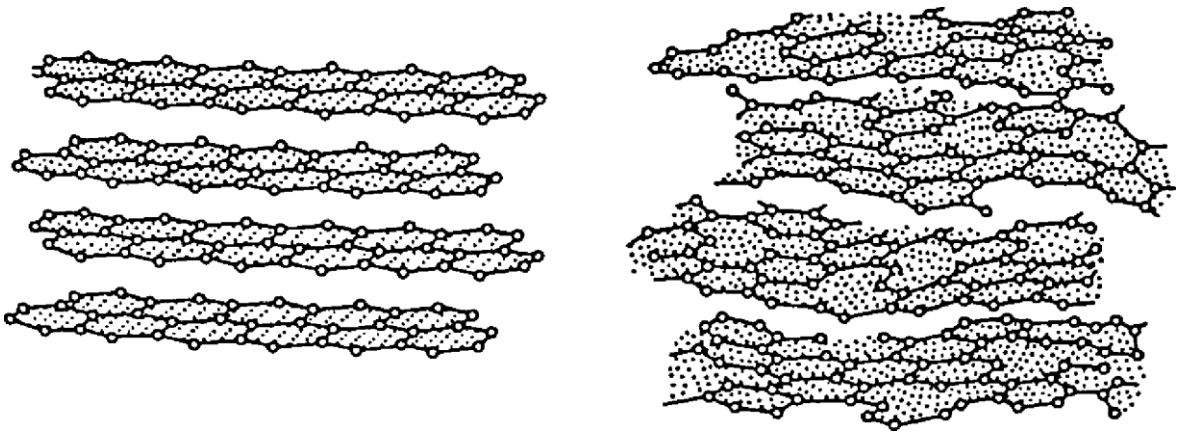

(a) (b)

Figure 2.3 Comparison of three-dimensional crystal lattice of graphite (a) and the activated carbon structure (b) (Bansal and Goyal, 2005)

In addition to sulfur, nitrogen and halogens, activated carbons possess considerable amount of hydrogen and oxygen. These molecules have either devised from the starting material or they chemically bonded to the activated carbons during carbonization activation or any other treatment. X-ray diffraction studies revealed that these hetero atoms are bonded to the edges and corners of the aromatic sheets as well as to the defect positions, and forming carbon-oxygen, carbon-hydrogen, carbon-halogen, carbon-nitrogen

and carbon-sulfur surface compounds, which are generally called surface functional groups. These functional groups have a strong influence on the acidity and basicisity character of the activated carbons and on the adsorption properties as well. (Bansal and Goyal, 2005)

Oxygen bearing surface groups are by far the most important groups on activated carbons. They affect the acidity characteristics as well as wettability and polarity. They are formed by chemisorption of molecular oxygen to the defected sites of the lattice structure. High temperatures favors dissociation of the oxygen atoms, thus, has a positive effect on the formation of these groups However, gasification and the decomposition of the carbon structure begins above 400 °C in the presence of O_2. By using oxidizing gases such as ozone, nitrous oxide, nitric oxide, carbon dioxide, etc.. and oxidizing solutions like nitric acid, sodium hypochlorite, hydrogen peroxide, etc.., it is possible to change the types and abundance of surface complexes. There are several oxygen surface groups as illustrated in the Figure 2.4. (Rodriguez-Reinoso and Molina-Sabio, 1998).

There are three types of carbon oxygen surface groups namely acidic, basic and neutral. Acidic groups are well recognized and they are formed on the surface by oxygen treatment up to 400 °C as well as treating with oxidizing solutions at room temperature. They are hydrophilic and polar in character. Carboxylic, lactone, and phenolic groups are acidic groups. These groups are thermally less stable and decompose in vacuum or an inert atmosphere between 350-700 °C emitting CO_2. Neutral surface groups decomposes to CO_2 upon heat treatment as well, however they are more stable and start to decompose at 500-600 °C and they require heating up to 950 °C for complete decomposition. Neutral surface groups are formed when oxygen atoms are irreversibly chemisorbed, on the activated carbon surface at the ethylene type unsaturated sites (Bansal-Goyal, 2005).

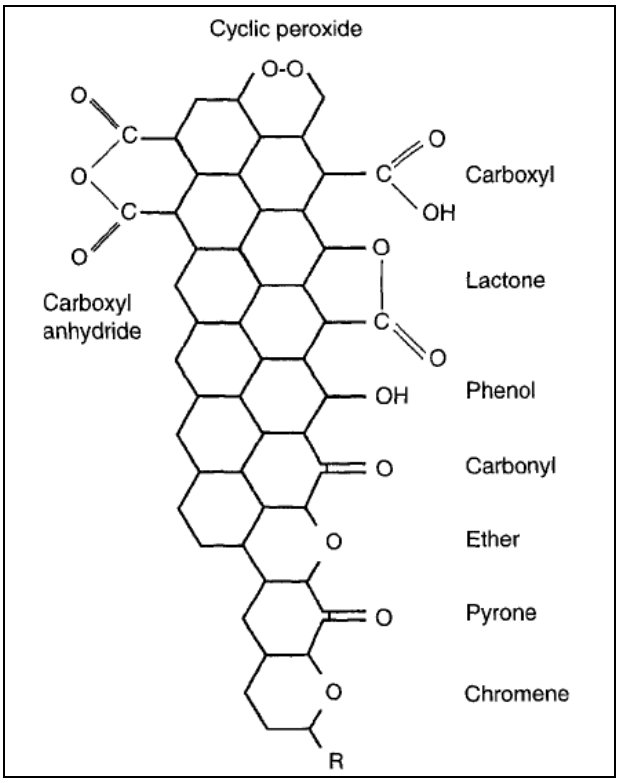

Figure 2.4 Structures of oxygen functional groups on carbon surfaces (Rodriguez-Reinoso and Molina-Sabio, 1998).

Basic surface groups, on the other hand, are not fully recognized. In order to introduce a basic character to an activated carbon, first it is outgased at temperatures higher than 700 °C and then cooled down to room temperature in an oxygen free environment and finally exposed to oxygen. Following these treatments, activated carbons show basic character in water. The basic character is attributed to the graphene layers containing most of the π electrons, which binds protons and H_3O^+ molecules (March and Rodriguez-Reinoso, 2006).

Different oxidation treatments results in different types of oxygen groups. Moreno-Castilla *et al*. (2000) treated activated carbon samples with H_2O_2 (H treatment), $(NH_4)S_2O_2$ (S treatment), HNO_3 (N treatment) and studied the samples by using XPS and FTIR techniques. It was found out that the amount of oxygen bearing surface groups have increased mostly in the N treated samples, whereas on the treated samples with H and S the functional groups have formed only on the external surface. Although limited amount of

oxygen bearing surface groups were fixed on the surfaces of S treated samples, they show the most acidic character upon titration with NaOH and HCl. S treated samples gave the highest product (di-methyl ether) yield in catalytic decomposition of methanol tests used as a probe reaction, proving high surface acidity.

In a similar study on activated carbon supports and AC supported catalysts by Aksoylu *et al*. (2001), it was found that air and HNO_3 oxidation change the surface chemistry of the AC samples significantly; the change in surface chemistry results in higher dispersion of Pt metallic sites on AC supported Pt/AC catalysts, although both air and HNO_3 oxidation decreased the surface area of AC samples. In the study, HNO_3 oxidation gave rise mostly to acidic groups namely carboxylic acid and anhydrides. The air treatment on the other hand has removed all the carboxylic acids and half of the anhydrides, whereas increased lactone groups. In general, HNO_3 treatment resulted in an increase in acidic character and air treatment increased basic character of the activated carbon samples.

The raw materials used as well as the preparation procedure applied in the production of original activated carbon samples is another important parameter that affects the surface chemistry of furtherly oxidized carbon supports. Even though there is a huge difference in the increase of phenolic groups of original Norit ROX samples with two oxidation methods (9 folds increase with HNO_3 treatment, 2 folds increase with air oxidation) the increases in these groups were similar for both oxidation methods on hydraffine samples. In contrast, HNO_3 treatment increased high temperature carbonyl-quinone groups significantly whereas this increase is rather limited for Norit ROX samples (Aksoylu *et al*., 2001).

2.2.3. Surface Chemistry Characterization

Widely used methods in characterization of surface functional groups can be divided into four categories, namely: Temperature programmed decomposition, neutralization of alkalies, specific chemical reactions and spectroscopic methods. Temperature programmed desorption (or Temperature Programmed Surface Group Decomposition) studies (TPD or TPSGD) will be explained in detail in section 2.2.3.1.

Alkali neutralization is one of the oldest methods in characterization of the surface groups on carbon based materials. It is based on the selective neutralization of surface acidic groups; for instance, carboxyl groups react with sodium ethoxide but not with sodium hydroxide. Similarly weak acidic groups that react with NaOH but not with Na_2CO_3 were attribute to phenol groups and the strong acids that are neutralized by $NaHCO_3$ but not by Na_2CO_3 were postulated as lactones. Although there is an argument about the validity of this technique, neutralization results are in agreement with the thermal desorption studies to a large extend in the literature (Bansal and Goyal, 2005).

Although not applicable to all surface groups, specific chemical reactions is a direct method in determination of surface functional groups such as carboxyls, lactones, phenols and quinones. Methylation of the carbon with diazomethane followed by hydrolysis of the methylated product with a mineral acid is a common method in organic chemistry. Hydrolyzed part has been attributed to carboxylic groups and to lactones, whereas unhydrolyzed portion was attributed to phenolic groups. Quinons are investigated by reduction with sodium borohydride (Studbaker *et al*., 1956; Bansal-Goyal, 2005).

Various spectroscopic methods that utilize diffraction of light and sound are used in the surface characterization of the activated carbons, namely; infrared spectroscopy (IR), electron spin resonance (ESR), transmission-absorption infrared spectroscopy (IR-T/A), fourier transform infrared spectroscopy (FTIR), photoacroustic spectroscopy (PAS) photothermal beam deflection (PDS) and X-ray photoelectron spectroscopy (XPS).

2.2.3.1. Temperature Programmed Desorption (TPD) Studies. Temperature programmed desorption is the most widely used method in estimation of the type and the quantity of surface functional groups on activated carbon samples. Technique is based on heating AC samples up to 1000 °C in an inert atmosphere or vacuum. Surface groups are decomposed into CO, CO_2 or both at certain temperatures based on their thermal stabilities. Then, through the analysis of the desorbed gas, it is possible to estimate the oxygen bearing surface groups. There is a debate on the decomposition temperature of the surface groups nevertheless the temperature ranges that were attained are quite similar in previous works. Figueiredo *et al.* (1999) reviewed and summarized these decomposition temperature ranges in a comprehensive figure (Figure 2.5).

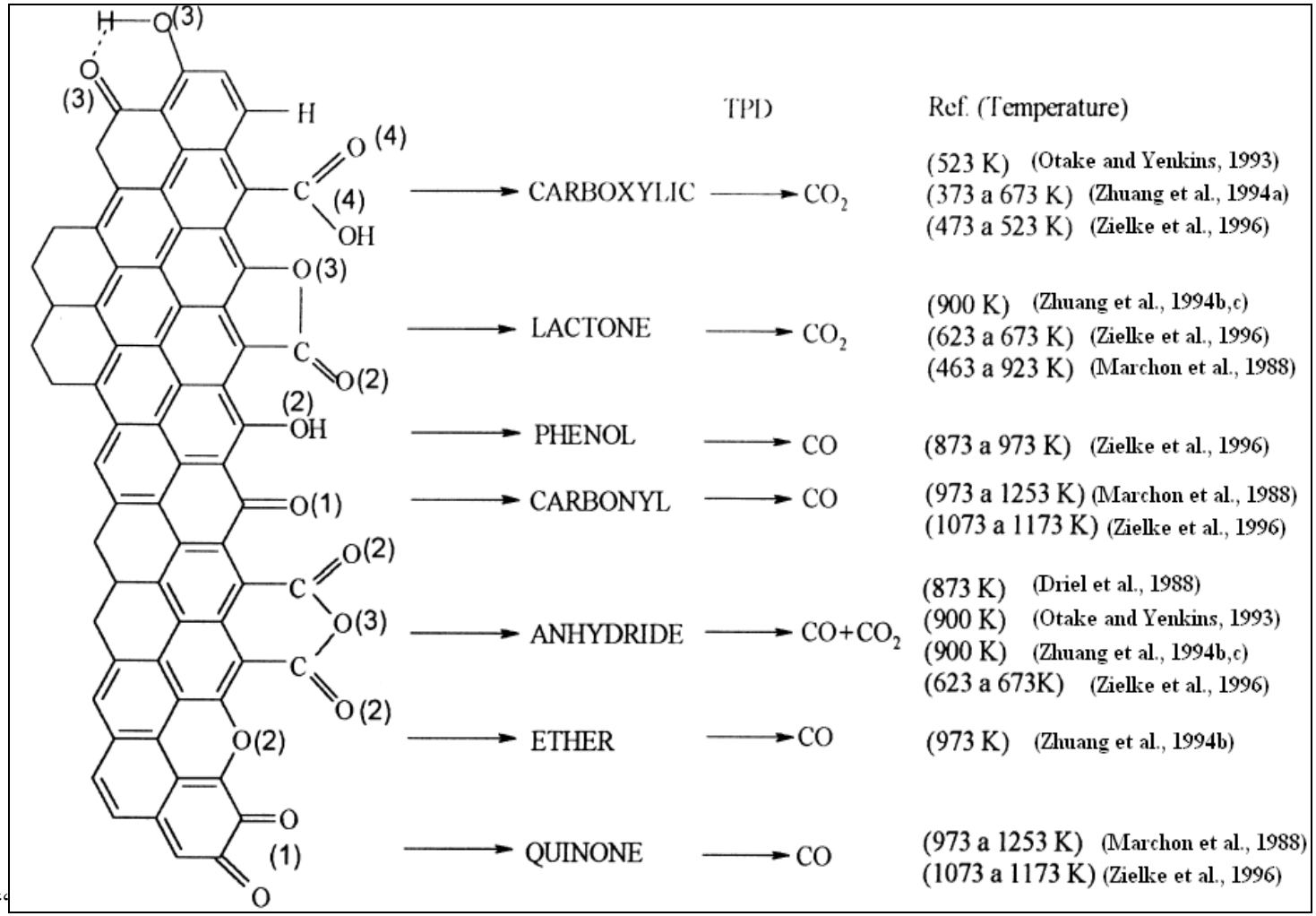

Figure 2.5 Surface groups on carbon and their decomposition by TPD (Figueiredo *et al.*, 1999)

Temperature ramp rate and inert flow rate is also important key points in TPD/TPSD studies. To prevent secondary reactions between desorbed CO and active sites, heating rate should be kept low (≤5 °C/min) and inert flow rate should be adjusted to a high degree (> 20 ml/min). By this way concentration of CO trapped in micropores upon decomposition is maintained low. (Aksoylu *et al.*, 2001)

2.3. AC as CO_2 Adsorbent

Increase in the emission gas concentration in the atmosphere is a major problem concerning the climate changes, which threatens life on earth. Removal of carbon dioxide from effluent gas streams with solid adsorbents is an effective way of reducing CO_2 emissions.

The success of removal of CO_2 by adsorption depends on utilization of low cost adsorbents, which has high CO_2 selectivity and cyclic adsorption/desorption operations without any loses in adsorption capacity. ACs are promising candidates to be used in CO_2 adsorption considering their low production cost, high moisture resistance, high CO_2 adsorption capacity at ambient pressure and, easy regeneration (Plaza *et al.*, 2009). A study by Pellerano *et al.* (2009) revealed that on a volume of the adsorbent basis, zeolite adsorbents have a higher adsorption capacity due to the higher density of zeolites in comparison to AC. However on a mass basis, AC have higher adsorption capacities at higher pressures (>2 bar). Additionally ACs endure better during cyclic operation: In their study adsorption capacity of AC sample remains unchanged even after 15th cycle whereas the zeolite adsorbents have lost their adsorption capacity by 40 % after 3rd cycle (Pellerano *et al.*, 2009).

2.3.1. CO_2 Adsorption for Purification of H_2 in PEM Fuel Cells

Hydrogen is often referred as a clean energy source. Producing hydrogen from natural gas on the other hand, leads to formation of impurities, like CO, CO_2 and CH_4 in the H_2 rich product stream. Considering the fact that, even a trace amount of CO (10 ppm) is enough to poison the Pt anode of proton exchange membrane (PEM) type fuel cell, CO in the hydrogen stream must be eliminated. In order to get rid of the CO impurity in a fuel

processor, preferential CO oxidation (PROX) takes place after the water gas shift (WGS) reactions which convert CO into CO_2 while increasing H_2 concentration through utilizing hydrogen coming from water. Although CO_2 is considered as an inert gas, studies revealed that CO_2 may lead to formation of CO via reverse water gas shift reaction (Bruijn *et al*., 2002). As a result, in addition to withdrawal of CO, removal of CO_2 is important in both preventing PEM fuel cell poisoning and for reducing CO_2 emissions into the atmosphere.

Chlendi and Tondeur (1995) used AC and zeolite adsorbents respectively, in their two bed Pressure Swing Adsorption (PSA) system in order to purify H_2 coming from a typical WGS reaction product gas, which contains 71-75 % H_2, 15-20 % CO_2, 4-7 % CH_4, 1-4 % CO and 1 % N_2. As zeolite irreversibly adsorbs CO_2, in order to achieve a reversible adsorption system, all the CO_2 in the stream should be adsorbed by AC bed which has selective and reversible CO_2 and CH_4 adsorption ability. In the study, by using a two bed system where CO_2, CH_4 is adsorbed on AC and CO, N_2 is adsorbed on zeolite, 99.999% pure hydrogen stream was obtained.

In a similar study, Majlan *et al*. (2009) used AC to adsorb CO_2 and CO in order to purify hydrogen for fuel cell systems. In their research, they used a commercial AC adsorbent from Sigma–Aldrich in their PSA system and managed to reduce the CO_2 concentration from %5 to 7.0ppm and CO from 4000 ppm to 1.4 ppm in a gas mixture of H_2/CO_2/CO for 3600s and 60 cycles.

2.3.2. Modifications on AC to increase CO_2 Adsorption Capacity

Literature shows that, CO_2 adsorption capacity of the activated carbons can be altered by surface chemistry modification. It is well acknowledged that CO_2 is a Lewis acid thus increase in the AC basicity have a positive effect on CO_2 adsorption. It is suggested that one way to alter the CO_2 adsorption capacity is to increase bacisity by heat treatment with gaseous ammonia instead of CO_2 activation. In fact, ammonium treatment increases CO_2 capacity of AC samples significantly by introducing nearly 5 % nitrogen, which is incorporated in pyridine and pyrrol-type functionalities on the surface (Plaza *et al.,* 2009a,b). These nitrogen functional groups are thought to be formed mostly by reaction of NH_3 with carboxylic acids. HCN and NH_3 profiles in the TPD studies revealed

that at least 4 different nitrogen functionalities have formed on the surface affecting adsorption capacity differently (Pevida *et al.,* 2008). The studies revealed that pore size distribution and surface chemistry are more important parameters than the surface area of the AC adsorbents in CO_2 adsorption at low relative pressures (Plaza *et al.,* 2009b).

Another way to modify surface chemistry of AC is impregnation. Slurry and solution impregnation techniques are widely used on activated carbon samples aiming to prepare AC supported catalysts as well as AC based adsorbents having enhanced adsorption capacities. Pore blockage and thus a decrease in the surface area of the samples are common problems reported. Washing step after impregnation is highly desired in order to prevent blockage of the pores by impregnation. It was reported by Somy *et al.,* (2009) that CO_2 adsorption capacity can be increased up to 25 % by slurry impregnation of both Cr_2O and zinc carbonate hydroxide on the activated carbons.

2.4. AC as Butane Adsorbent

The possibility of undergoing chemical reactions forming ozone depleting species and potential adverse health effects makes volatile organic compounds, such as butane, a danger for the environment and their emissions are regulated very stringently. Solid adsorbents such as activated carbons, alumina, graphite powders and carbon blacks and zeolites are used as butane adsorbents for separation and purification purposes (Diaz *et al.*, 2004).

The main advantage of carbon materials especially AC, is that they have nanoporous structure which leads to high surface area. Studies conducted by Mangun *et al.*, (1998) have revealed the correlation between pore size distribution of activated carbon fibers and their adsorption capacity for light hydrocarbons. Based on the study, the lower surface area (smaller pore size) materials had higher adsorption capacities for low boiling point gases/vapors and contaminants at low concentrations. For higher boiling point gases/vapors and contaminants of higher concentrations on the other hand, the adsorption capacity was higher for higher surface area materials (larger pore size) due to larger pore volumes.

Correlation between high adsorption capacity and high porosity is also acknowledged by Saha *et al.* (2008); as high as 71 % weight increase has been reported at 298.15 K and 1 bar for pure butane adsorption on a commercial, high surface area (3140 m^2/g) pitch base activated carbon adsorbent (Maxsorb III, manufactured by Kansai Coke and Chemicals Co. Ltd., Osaka, Japan).

Expectedly, some researchers argue that adsorption capacity is related not only with the textural properties, such as surface area, pore size and structure, but also with the surface chemistry. Samples with similar pore sizes and surface areas exhibit different butane adsorption properties based on their surface chemistry (Yenisoy-Karakaş *et al.*, 2004).

A key concept in the butane adsorption on activated carbon is butane working capacity (BWC). The BWC, is a well established test method and is a measure of the ability of activated carbon to adsorb and desorb butane from dry air under specified conditions. There, the butane activity used as an indication of cyclic adsorption capacity and given as gram of reversibly adsorbed butane per 100 ml of the adsorbent (Allan *et al.*, 1999, Yenisoy-Karakaş *et al.*, 2004).

2.4.1. Evaporative Emission Control with Carbon Canisters

Evaporation loses from gas tanks of vehicles are considered as the highest source of hydrocarbon emissions on road transport. Fuel volatility, design of the vehicle, ambient temperature and temperature variation, and driving conditions are the four major factors that effect evaporative emissions (Mellios and Samaras, 2007). To reduce hydrocarbon emissions, a canister is used at the purge exit of the tanks to adsorb hydrocarbon vapors reversibly. Activated carbons are used as the main adsorbents in canister beds owing to high stabilities and adsorption capacities.

There are certain test methods for the capacity and permeability of the carbon canisters. One standard method as European Commissions (1998) has approved includes studying hydrocarbon emissions by increasing, the temperature of a 40% filled tank with a rate of 1 °C in 9 minutes repeatedly until the breakthrough, which is defined as emission of

2 g of hydrocarbon, occurs. Then the canister is purged with 25±5 l/min air. This loading and purging is continued until weight of the canister stabilizes after the purge step. Before soak and diurnal tests, carbon canisters are loaded with butane at a rate of 40 g /hour butane by using a 50 % air 50 %butane mixture.

To test their model for canister behavior and breakthrough, Lavole *et al.*, (1996) has performed experiments in which they used butane to represent fuel vapor. In the study, the canisters were loaded with 50 % butane, 50 % N_2 mixture with a flow rate of 40 g/hr butane as the base case. In order to validate the model further, varying concentrations of butane and N_2 mixtures were sent until break through occurs. Heat of adsorption and canister heating were also measured and recorded in the study. On a similar study by Mellios *et al.* (2009), the importance and effect of purging was mentioned in the context that the effective adsorption of the vapors generated is provided by well purged canisters.

3. EXPERIMENTAL WORK

3.1. Materials

3.1.1. Gases/Liquids

All the gases were produced by Birleşik Oksijen Sanayi (BOS). Details of the gases used in the study for calibration, adsorption and characterization purposes are summarized in Table 3.1.

Table 3.1 Purity, provider and application of gases/liquids used in the study.

Gas/Standard	Purity	Provider	Application
Helium	99.999%	BOS	DSMS calibration, TPD, selective CO_2 adsorption, BET carrier
Butane	99.999%	BOS	Butane Isotherms, Canister testing
Carbon dioxide	99.999%	BOS	CO_2 Isotherms, selective CO_2 adsorption, DSMS calibration
Carbon monoxide	99.999%	BOS	Selective CO_2 adsorption, DSMS calibration, canister testing
Hydrogen	99.99%	BOS	Selective CO_2 adsorption, DSMS calibration
Nitrogen	99.999%	BOS	Canister testing, BET
Nitrogen (Liquid)	99%	HABAŞ	BET cold trap

3.1.2. Activated Carbon Samples

Three types of commercial activated carbon samples for butane adsorption studies (AC10, AC11 and AC12) were obtained from Ford Otosan A. Ş. Samples for selective CO_2 adsorption studies were prepared based on a commercial activated carbon Norit ROX kindly provided by Norit and the treatments are summarized in Table 3.2. Detailed

descriptions of the treatments are explained elsewhere (Aksoylu *et al*., 2000). The alkali treated samples were prepared by B. S. Çağlayan.

Table 3.2. Treatments on the AC samples used for CO_2 adsorption

Name	Description	Mesh Size	Treatment
AC0	Norit ROX	-	-
AC1	HCl washed Norit ROX	200-300µm	Grinded sample was refluxed with 200mL 2 N HCl for 12 h, washed with distilled water for 6 h. Overnight dried at 115 °C.
AC2	HCl washed and air oxidized Norit ROX	200-300µm	AC1 is air oxidized at 450°C under 150 mL/min N_2 and 50 mL/min dry air
AC3	HCl washed and HNO_3 oxidized Norit ROX	200-300µm	AC1 is oxidized with 5 N HNO_3 for 3 h, then rinsed till pH 5.5 has been reached and dried overnight
AC4a	Na_2CO_3 impregnated and calcined (300 °C) AC2	200-300µm	AC2 is impregnated with 10 % Na_2CO_3, dried overnight at 105°C and calcined at 300 °C under 150mL/min N_2 and 50mL/min air for 2 h
AC4b	Na_2CO_3 impregnated and calcined (200 °C) AC2	200-300µm	AC2 is impregnated with 10 % Na_2CO_3, dried overnight at 105 °C and calcined at 200 °C under 150mL/min N_2 and 50mL/min air for 2 h
AC4c	Na_2CO_3 impregnated and calcined (250 °C) AC2	200-300µm	AC2 is impregnated with 10 % Na_2CO_3, dried overnight at 105 °C and calcined at 250 °C under 150mL/min N_2 and 50mL/min air for 2 h
AC5a	Na_2CO_3 impregnated and calcined (175 °C) AC3	200-300µm	AC3 is impregnated with 10 % Na_2CO_3, dried overnight at 105 °C and calcined at 175 °C under 150mL/min N_2 and 50mL/min air for 2 h
AC5b	Na_2CO_3 impregnated and calcined (200 °C) AC3	200-300µm	AC3 is impregnated with 10 % Na_2CO_3, dried overnight at 105 °C and calcined at 200 °C under 150mL/min N_2 and 50mL/min air for 2 h
AC5c	Na_2CO_3 impregnated and calcined (250 °C) AC3	200-300µm	AC3 is impregnated with 10 % Na_2CO_3, dried overnight at 105 °C and calcined at 250 °C under 150mL/min N_2 and 50mL/min air for 2 h

3.2. Experimental Setups and Procedures

3.2.1. Butane Adsorption Isotherms

The aim of the butane adsorption experiments were to test the adsorption capacity and to obtain adsorption-desorption profiles of activated carbon samples, which are used in the carbon canisters in automobile gas tanks. The use of butane to mimic the vapor behavior in the gas tanks is well established in the literature (Lavole *et al.*, 1996).

Butane adsorption isotherms were obtained for samples AC10, AC11 and AC12 by using Gravimetric Analyzer system from Hiden Isochema Warrington, England (Intelligent Gravimetric Analyzer, IGA). In order to obtain isotherms, IGA was adjusted to static mode and butane cylinder was connected to IGA directly without using mass flow controllers. Data was stored in a PC. Experimental setup is shown in Figure 3.1.

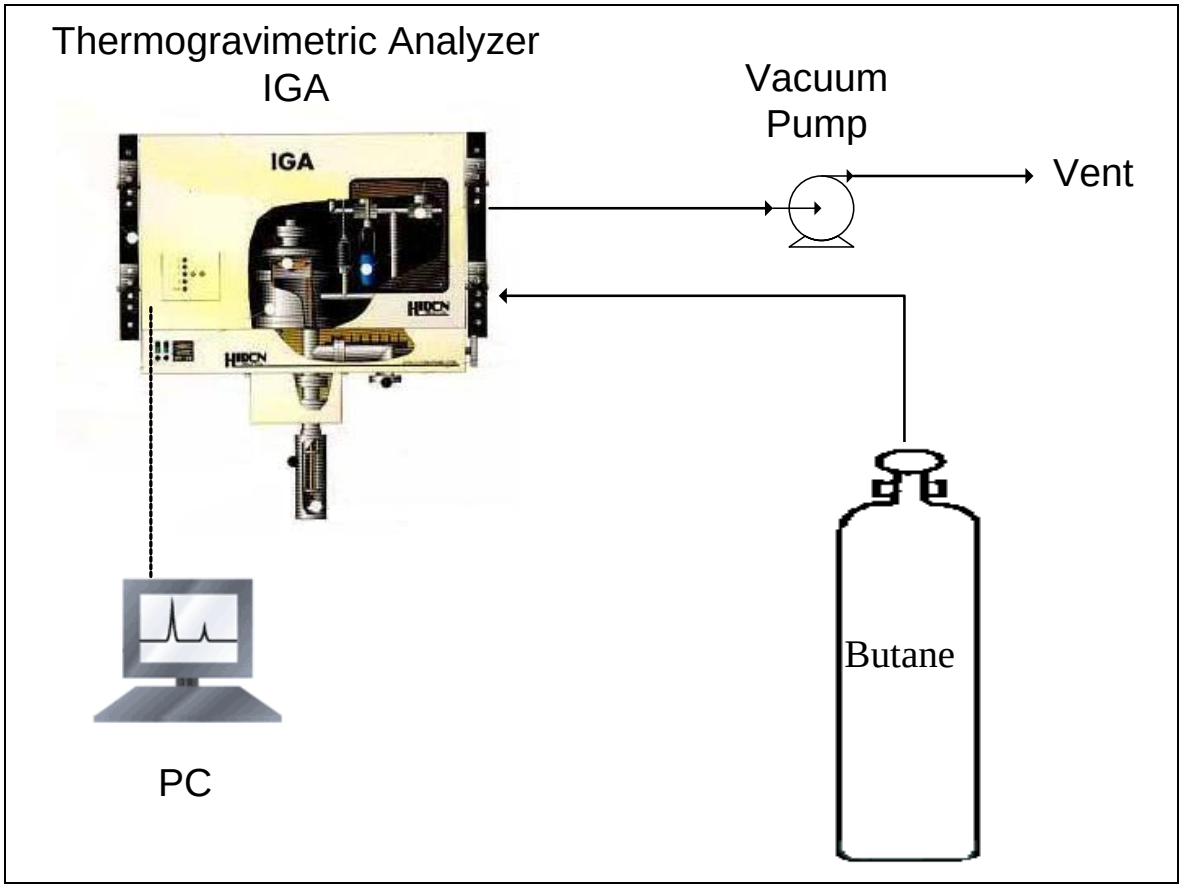

Figure 3.1 Experimental setup for Butane isotherms

Before adsorption runs, samples were outgased at 110°C overnight at a pressure $5x10^{-3}$mbar. In the adsorption tests, butane pressure was increased in 100mbars steps starting from zero ($5x10^{-3}$mbar) to 1300mbars by using a leak valve. In order to reach the system stability, it was waited for 20 minutes for each step before recording equilibrium adsorption capacity. Following the adsorption, butane pressure was decreased with 100mbars steps down to zero ($5x10^{-3}$mbar) and desorption profiles were established. Isotherms were obtained at 40 °C, 70 °C, and 100 °C by using fresh samples.

Cyclic adsorption ability for butane was also investigated on the samples AC10, AC11 and AC12. Ten cycles (4 at 40 °C, 3 at 70 °C and last 3 at 100 °C) were sequenced by utilizing IGA. Each cycle consisted of one adsorption and one desorption period. The adsorption and desorption procedures explained above were applied for each cycle.

3.2.2. Selective CO_2 Adsorption Studies

Selective CO_2 adsorption studies were conducted by using IGA apparatus in flow mode. Gas cylinders were connected to IGA via mass flow controllers (MFC) produced by Brooks Instruments. MFCs are calibrated by using soap bubble technique. Concentrations of the gases in the chamber were analyzed simultaneously by using a dynamic sampling mass spectrometer (DSMS, Hiden Analytical; Warrington, England) which was calibrated via using gas mixtures having different concentrations. The gas mixtures were prepared in a home-made mixing unit having MFCs and valve system. Data were stored in a PC. Experimental setup is shown in Figure 3.2.

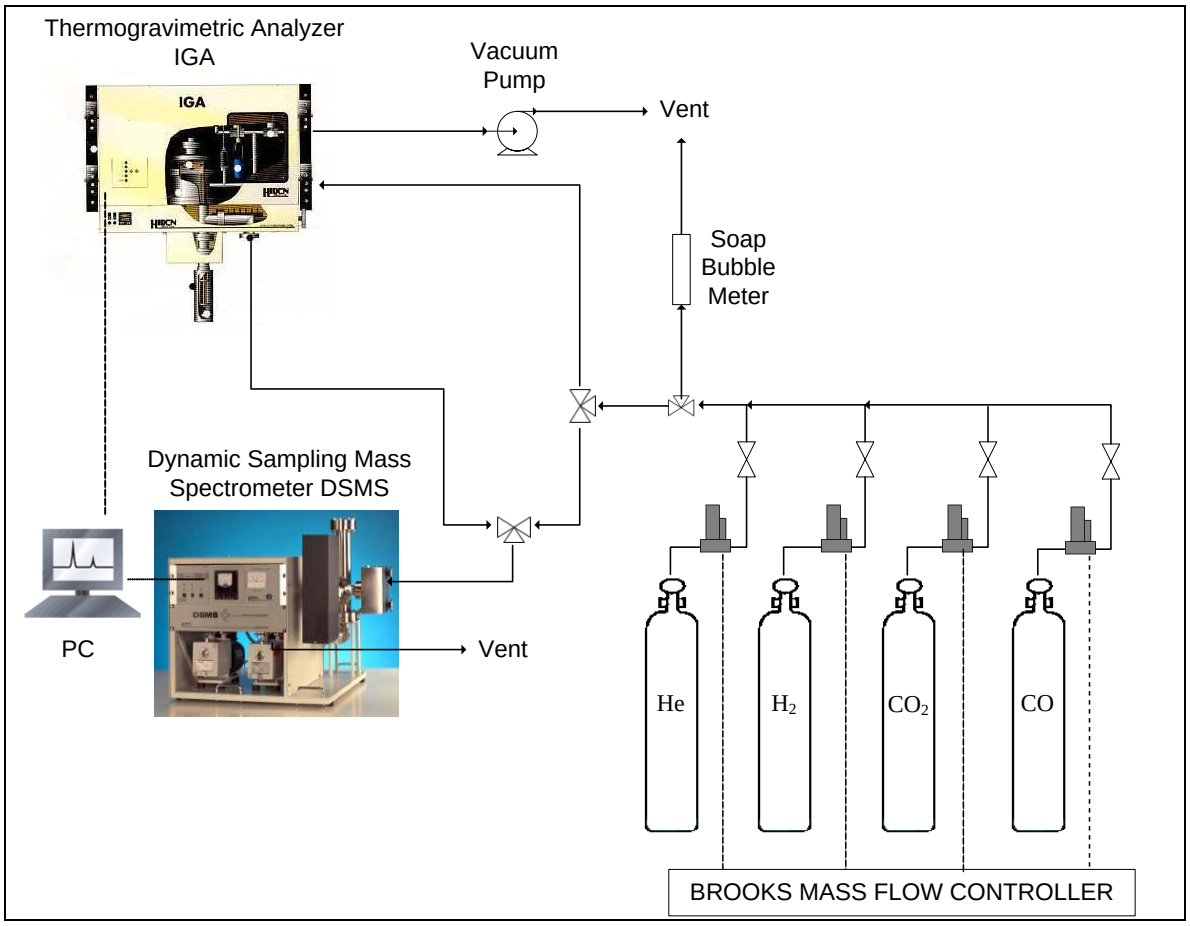

Figure 3.2. TPD and selective CO_2 adsorption test setup

Prior to adsorption studies, pretreatment was carried out in order to degas IGA chamber and to remove adsorbed species on the samples. Pretreatment steps are listed in Table 3.3.

Table 3.3 Pretreatment steps for Selective CO_2 adsorption experiments

	Pretreatment Steps
1	The chamber was outgased at room temperature with a rate of 80 mbar/min and was kept at $5x10^{-3}$mbar for 1 hour.
2	Chamber was filled with inert He with a rate of 200 mL/min till 1000 mbar pressure was established.
3	Chamber was heated to 110 °C with a ramp rate of 5 °C/min under 10mL/min He flow.
4	Chamber was outgased at 110 °C with a rate of 80 mbar/min and was kept at $5x10^{-3}$ mbar for 1 hour.
5	Chamber was filled with He with a rate of 200 mL/min till 1000 mbar pressure was established at 110 °C.
6	Gas flow was shut off and the chamber was cooled to room temperature.
7	Chamber was heated to 40 °C.

Selective CO_2 adsorption under dynamic conditions from a flow of mixture of H_2, CO, CO_2 and He was studied in the above mentioned apparatus and the concentration of each gas in the chamber was analyzed by using a quadropole dynamic sampling mass spectrometer (DSMS) as illustrated in Figure 3.2.

Concentrations in the gas mixture were determined in order to model a typical WGS reactor exit with the exception of methane and water. 200mL/min flow consisted of 50% H_2, 2% CO, 15% CO_2, and balance He (Soykal, 2008) was sent via calibrated MFC controllers. In order to observe selective adsorption behavior, gas stream without CO_2 was introduced to the system prior to the adsorption experiments until both the gravimetric analyzer readings and concentration profile in the system was stabilized. After stabilization was confirmed both with IGA and DSMS, CO_2 was introduced and the weight change of the sample during adsorption was recorded with gravimetric analyzer.

After the adsorption was completed, which was confirmed by stabilized weight of the sample, the cyclic adsorption behavior of the samples was determined via following shutting off CO_2 flow for nearly 1 hr for desorption and then reestablishing the CO_2 after the desorption period, for the second cycle.

3.2.3. Textural Characterization via N_2 Adsorption

Surface area measurements were conducted by adsorption of N_2 with varying partial pressures via Micrometrics Flowsorb II 2300 instrument. Data were taken in the 0.05-0.25 P/P_0 range by adjusting N_2 concentration in He between 5-25%.

Before N_2 adsorption measurements, samples were dried and degassed under He flow at 523 K for 2.5 h. Before each run, Flowsorb 2300 was calibrated by injecting 1mL N_2 gas in the ambient conditions, adjusting the machine to the corresponding adsorbed volume and setting the instrument to indicate adsorbed and desorbed volumes in standard conditions thereafter.

In the experiments, flow of a mixture of N_2 and He in varying concentrations (5-25% N_2 in He) was introduced to the samples, which were kept at liquid nitrogen temperature (77 K). Then, the temperature of the samples was raised to the ambient temperature. Both adsorption and desorption data were measured by a thermal conductivity detector. This procedure was repeated at least four times with different N_2 and He concentrations aiming to construct the BET isotherm.

3.2.4. Surface Characterization via TPD

Oxygen bearing surface groups were determined for samples: AC10, AC11, AC12, AC0, AC1, AC2 and AC3 by using TPD method which was specifically called as Temperature Programmed Surface Group Decomposition (TPSGD). TPD was carried out in the same experimental setup which was used for selective CO_2 adsorption studies. The setup is explained in section 3.2.2 and Figure 3.2 in detail.

Nitrogen in air which was introduced in the chamber during sample load can easily deceive the CO reading in the mass spectrometer; thus, the chamber should be properly degassed prior to the TPSGD studies. In the experiments, IGA chamber was outgased twice by following the procedure that was explained in section 3.2.2 up to step 5, in order to remove nitrogen in the chamber and to desorb any adsorbed species on the samples. After 5^{th} step, the chamber pressure was maintained at 1000mbars and 200mL/min He flow

was maintained for nearly one hour. Prior to the experiments, less than 15 ppm CO noise (baseline) was validated by using DSMS.

TPSGD studies were carried out under 200mL/min He flow in 1000mbar. The reason behind the high He flow rate is to reduce space time in the IGA chamber, aiming to shorten the tails of the deconvoluation peaks. To validate the applicability of flow rate, a CO_2 pulse was given to the chamber and it was observed that CO_2 concentration was reduced to one hundredth in 5 minutes under 200mL/min He flow.

In the TPD experiments, temperature was increased from 110 °C to 950 °C with a rate of 1.872 °C per minute in order to prevent any secondary formation or adsorption of CO in the decomposed surface sites. This procedure aims to keep CO concentration trapped in the micropores as low as possible. CO_2 and CO decomposition was measured dynamically with DSMS and recorded at PC as well as the gravimetric readings from IGA.

4. RESULTS AND DISCUSSION

4.1. Sample Characterization

4.1.1. Textural Characterization via BET

Total surface areas of the samples AC10, AC11 and AC12 were determined via the BET method by using eq. 2.3 and 2.2. A straight line was plotted on $P/V(P_0-P)$ vs P/P_0 graph from the N_2 adsorption (at 77K) data with the help of the software supplied by Micromeritics Inc. together with the Flowsorb unit. Total surface areas of the samples are given in Table 4.1.

Table 4.1 BET surface areas of AC10, AC11 and AC12

Sample	BET (m^2/g)
AC10	1147.2
AC11	1100.95
AC12	1773.8

Textural characterization of samples AC1, AC2 and AC3 was performed previously by Aksoylu *et al.* (2000) and the results are summarized in Table 4.2.

Table 4.2 Surface areas of Norit ROX based activated carbons (Aksoylu *et al.*, 2000)

Sample	Oxidation	BET (m2/g)
AC1	None	1058
AC2	Air	1273
AC3	HNO_3	984

It is seen that air oxidation increases the pore size thus the surface area whereas HNO_3 treatment has an inverse effect on surface area possibly due to collapsing of micropore walls during the heat treatment in the acidic environment (Aksoylu *et al.*, 2000).

4.1.2. Surface Chemistry Characterization via TPD/TPSGD

Degassed activated carbon samples were heated from 373 to 1223 K under He flow. Desorbed CO and CO_2 were recorded with DSMS. CO_2 profile was decomposed into three Gaussian peaks in order to estimate the types and abundance of surface groups. Low temperature (510 – 620 K) surface group was estimated as carboxylic groups, whereas mid temperature (610-850 K) desorption of CO_2 was attributed to decomposition of anhydrides and high temperature (750-1050 K) CO_2 desorption to lactones. Similarly, CO desorption profile was decomposed to three Gaussian type peaks representing surface group decomposition, namely anhydride (610-910 K), phenol (940-1045 K) and carbonyl-quinone (1081-1190 K) groups. Peak temperature and the width of the Gaussian peaks were determined by using a Matlab code written by H. Bedir, which utilizes non linear optimization sequence in order to reduce the discrepancy between the sums of the deconvoluted peaks and desorption data. Initial guess and constraints for peak widths and peak temperatures were determined upon investigating parameters used in the literature (Aksoylu *et al.*, 1999; Figueiredo *et al.*, 1999). Same amount of CO and CO_2 decompositon from anhydride group was assumed and imposed as a constraint in the Matlab code. Summary of the decomposed groups for AC samples are given in Table 4.3 and 4.4. Deconvolution of AC1 is given in Figure 4.1 as an example; the other related figures are given in Appendix A, Figures A.1-A.7.

Table 4.3 Results of the deconvolution of TPD spectra for the Norit ROX based CO_2 adsorbent activated carbons using a multiple Gaussian function

	CO_2 Peak Deconvolutions									**CO Peak Deconvolutions**								
	Carboxyl			**Anhydride**			**Lactone**			**Anhydride**			**Phenol**			**Carbonyl-Quinone**		
Sample	**Area** *µmole/g*	**Peak T.** *K*	**Width** *K*	**Area** *µmole/g*	**Peak T.** *K*	**Width** *K*	**Area** *µmole/g*	**Peak T.** *K*	**Width** *K*	**Area** *µmole/g*	**Peak T.** *K*	**Width** *K*	**Area** *µmole/g*	**Peak T.** *K*	**Width** *K*	**Area** *µmole/g*	**Peak T.** *K*	**Width** *K*
AC0	108	526	132	94	700	202	61	876	250	94	850	202	180	1000	160	197	1131	128
AC1	74	513	107	42	610	80	97	755	250	41	610	80	505	980	300	257	1134	151
AC2	54	520	123	118	765	215	40	950	179	118	786	215	506	939	200	747	1080	199
AC3	1053	530	120	1496	700	225	199	949	171	1496	793	225	3029	977	200	303	1186	103

Table 4.4 Results of the deconvolution of TPD spectra for the Butane adsorbent activated carbons using a multiple Gaussian function

	CO_2 Peak Deconvolutions									**CO Peak Deconvolutions**								
	Carboxyl			**Anhydride**			**Lactone**			**Anhydride**			**Phenol**			**Carbonyl-Quinone**		
Sample	**Area** *µmole/g*	**Peak T.** *K*	**Width** *K*	**Area** *µmole/g*	**Peak T.** *K*	**Width** *K*	**Area** *µmole/g*	**Peak T.** *K*	**Width** *K*	**Area** *µmole/g*	**Peak T.** *K*	**Width** *K*	**Area** *µmole/g*	**Peak T.** *K*	**Width** *K*	**Area** *µmole/g*	**Peak T.** *K*	**Width** *K*
AC10	67	606	188	54	854	200	16	1062	133	54	824	200	655	1043	200	537	1188	83
AC11	75	642	262	55	898	87	28	1008	121	55	912	87	939	977	200	674	1188	119
AC12	92	597	202	86	887	200	3	1050	55	87	800	200	1122	965	200	267	1108	74

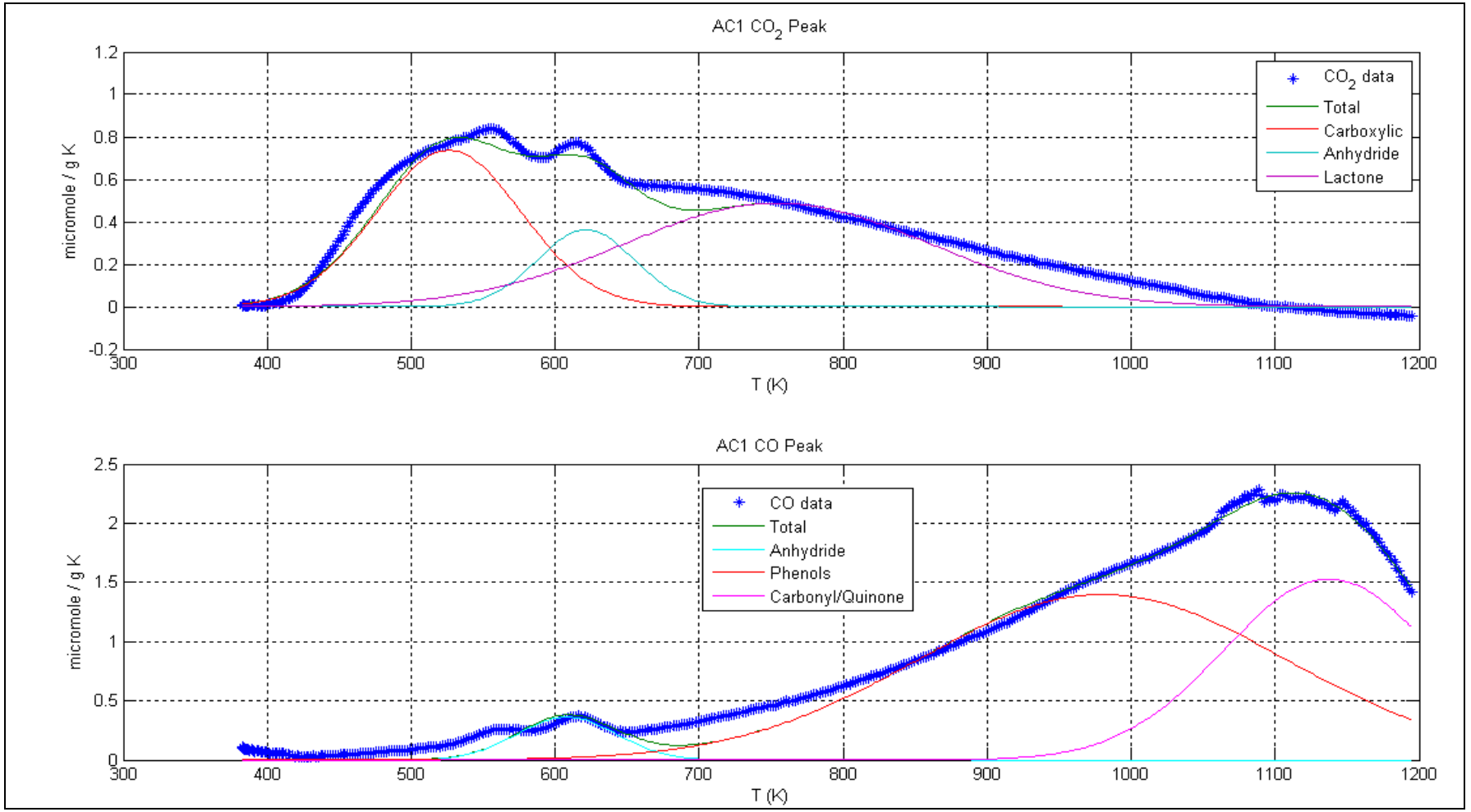

Figure 4.1. Deconvolution of TPD spectra of AC1

As it is seen from Table 4.3 HCl washing increased the amount of nearly all surface groups especially phenols with respect to untreated Norit ROX, whereas anhydride and carboxyl groups were reduced one half and one third, respectively. Air oxidation resulted in a slight increase in anhydrides and a significant increase in carbonyl/quinone groups, whereas the amount of lactones was decreased. Additionally, air oxidation removed some part of the carboxylic acid groups, which were presented in AC, in limited amounts. HNO_3 oxidation, on the other hand, had the most significant contribution on the oxygen bearing surface groups. Compared to AC1, AC3 had much higher carboxylic, anhydridic, lactonic and phenolic surface groups whereas surface area was not affected significantly. Per cent changes of surface groups and BET surface areas are summarized in Table 4.5.

Table 4.5 Per cent change in surface groups and surface area with air and HNO_3 oxidation with respect to HCl washed Norit ROX (AC1)

Treatment	**Carboxyl**	**Anhydride**	**Lactone**	**Phenol**	**Carbonyl-Quinone**	**BET**
Air	-27.5%	+183.2%	-58.9%	+0.3%	+190.1%	+20.3%
HNO_3	+1317.1%	+3489.3%	+105.2%	+499.6%	+17.8%	-7.0%

4.2. Selective CO_2 Adsorption Experiments under Dynamic Conditions

CO_2 adsorption capacity of the samples listed on Table 3.2 (AC0, AC1, AC2, AC3, AC4a, AC4b, AC4c, AC5a, AC5b, and AC5c) were investigated at 40 °C and 1000mbar in dynamic mode under a 200 mL/min gas mixture flow consisting 50% H_2, 2% CO, 15% CO_2 and balance He (by volume). CO_2 was introduced to the system when the samples were already in equilibrium with CO and H_2 flow. A typical concentration profile of CO_2 in the adsorption chamber, which was recorded with DSMS, is given in Figure 4.2. Weight increase due to adsorption was recorded with thermo gravimetric analyzer (IGA) and is shown in Figure 4.3. As it is easily recognized, weight increase is in accordance with the increase in the CO_2 concentration in the chamber.

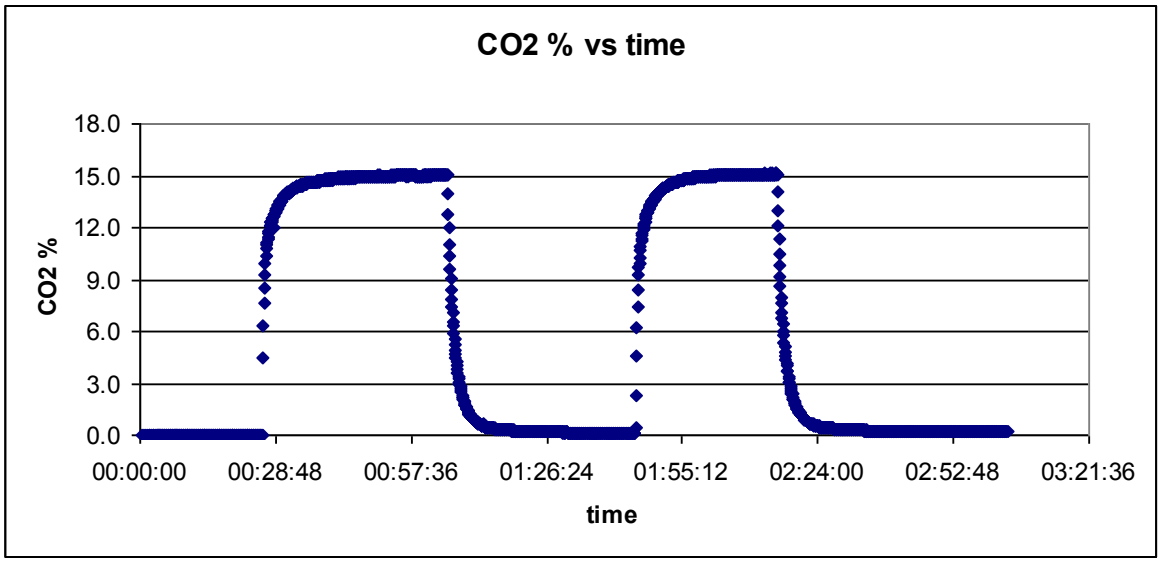

Figure 4.2 Typical CO_2 concentration profile in the adsorption chamber (Sample: AC2)

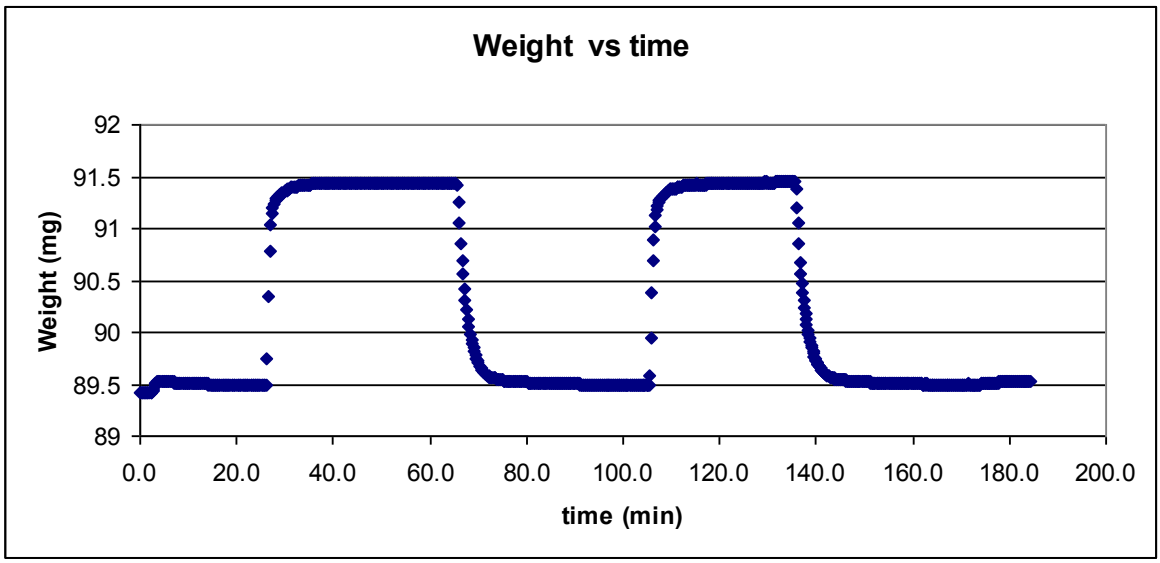

Figure 4.3 Weight change as a result of increase in CO_2 concentration (Sample: AC2).

Weight per cent adsorbed CO_2 and $CO+H_2$ on activated carbon samples was calculated according to equation 4.1 and 4.2 respectively.

$$A_{CO_2} = \frac{W_2 - W_1}{W_0} \cdot 100 \qquad (4.1)$$

$$A_{H2+CO} = \frac{W_1 - W_0}{W_0} \cdot 100 \quad (4.2)$$

where W_2 is the total weight of the sample measured at the end of the adsorption period when the CO_2 concentration became stable at 15%, W_1 is the sample weight prior to the CO_2 introduction (sample weight in equilibrium with H_2, CO and He), W_0 is the weight of dry sample under He flow, A_{CO2} is the weight percentage of adsorbed CO_2 to the dry weight of the sample and A_{H2+CO} is the weight percentage of adsorbed H_2 and CO to the dry weight of the sample. Results are summarized in Table 4.6.

Table 4.6 Weight per cent of adsorbed H_2+CO and CO_2

Sample	**W_0**	**W_1**	**W_2**	**AH_2+CO**	**ACO_2**
AC0	79.416	79.416	81.308	-0.001%	2.383%
AC1	82.559	82.618	84.508	0.071%	2.289%
AC2	79.577	79.639	81.569	0.077%	2.425%
AC3	77.743	77.773	79.296	0.039%	1.959%
AC4a	75.543	75.806	78.119	0.347%	3.062%
AC4b	87.982	88.172	90.661	0.216%	2.829%
AC4c	85.837	85.900	88.287	0.073%	2.781%
AC5a	83.443	83.725	86.376	0.337%	3.177%
AC5b	80.041	80.843	83.274	1.002%	3.036%
AC5c	81.632	81.990	84.821	0.438%	3.468%

4.2.1. Cyclic Adsorption Capacities

In the current study, the adsorption capacity after adsorption and desorption cycles, which is often referred as cyclic adsorption capacity, was also investigated. Adsorbed and desorbed CO_2 amount for first and second cycles were calculated with equation 4.1, 4.3 and 4.4.

$$D^1_{CO_2} = \frac{W_2 - W_3}{W_0} \cdot 100 \quad (4.3)$$

$$A^2_{CO_2} = \frac{W_4 - W_3}{W_0} \cdot 100 \quad (4.4)$$

$$D^2_{CO_2} = \frac{W_4 - W_5}{W_0} \cdot 100 \quad (4.5)$$

$$Adsorption\_loss = \frac{A_{CO_2} - A^2_{CO_2}}{A_{CO_2}} \cdot 100 \quad (4.6)$$

where, W_3 is the weight after first desorption, W_4 is the weight after second adsorption and W_5 is the weight after second desorption. The symbols D^1_{CO2}, A^2_{CO2} and D^2_{CO2} refers to the weight percentages of desorbed CO_2 in the first cycle, adsorbed CO_2 in the second cycle and desorbed CO_2 in the second cycle respectively. Adsorbed and desorbed CO_2 amounts for first and second cycles are summarized in Tables 4.7 and 4.8.

Table 4.7 Sample weights (mg) after adsorption cycles (W_3, W_4, W_5)

Sample	W_3	W_4	W_5
AC0	79.445	81.303	79.482
AC1	82.6745	84.539	82.717
AC2	79.643	81.566	79.650
AC3	77.746	79.265	77.734
AC4a	76.046	78.115	76.120
AC4b	88.441	90.658	88.483
AC4c	86.156	88.307	86.219
AC5a	84.377	86.449	84.547
AC5b	81.443	83.308	81.487
AC5c	82.881	84.956	83.108

Table 4.8 Adsorbed and desorbed CO_2 amounts by weight in first and second cycles

	First Cycle		Second Cycle		
Sample	A^1_{CO2}	D^1_{CO2}	A^2_{CO2}	D^2_{CO2}	**Adsorption Loss**
AC0	2.38%	2.35%	2.34%	2.29%	1.79%
AC1	2.29%	2.22%	2.26%	2.21%	1.35%
AC2	2.43%	2.42%	2.42%	2.41%	0.37%
AC3	1.96%	1.99%	1.96%	1.97%	0.20%
AC4a	3.06%	2.74%	2.74%	2.64%	10.57%
AC4b	2.83%	2.52%	2.52%	2.47%	10.92%
AC4c	2.78%	2.48%	2.51%	2.43%	9.86%
AC5a	3.18%	2.40%	2.48%	2.28%	21.85%
AC5b	3.04%	2.29%	2.33%	2.27%	23.28%
AC5c	3.47%	2.38%	2.54%	2.26%	26.71%

AC samples without Na_2CO_3 impregnation (AC0, AC1, AC2, and AC3) showed excellent cyclic behavior. Nearly all the adsorbed CO_2 were desorbed after 1 hour desorption period and cyclic capacity was reduced only less than 1.8%. However, Na_2CO_3 impregnated samples has lost 10-25% of their adsorption capacity after first adsorption cycle. Adsorption capacity of Na_2CO_3 impregnated air oxidized samples were reduced nearly 10%, whereas this decrease was 20-25% for impregnated HNO_3 treated samples.

4.2.2. Effect of Oxidation of AC on CO_2 Adsorption under Dynamic Conditions

Upon comparison of AC0 and AC1, it can be concluded that selective CO_2 adsorption capacity of Norit ROX was reduced by nearly 4% with HCl washing. Air oxidation treatment had a positive effect on both BET surface area and CO_2 adsorption capacity. Surface area has increased nearly 20% with air oxidation however increase in adsorption capacity is nearly 9%. HNO_3 treatment, on the other hand, has decreased both BET surface area and adsorption capacity. AC1 has lost 10.8% of its adsorption capacity upon HNO_3 treatment. The reason of this decrease can be explained both with 7% reduction in the surface area and with the change in the surface chemistry. As it can be followed from Table 4.3, HNO_3 treatment has introduced acidic surface groups namely

carboxyls, lactones and phenols to the activated carbon surface which may resulted in the repulsion of CO_2 which is considered as a Lewis acid (Plaza *et al.*, 2009a).

4.2.3. Effect of Na_2CO_3 Impregnation on Dynamic CO_2 Adsorption

It was seen that Na_2CO_3 impregnation on activated carbon has increased, CO_2 adsorption significantly, whereas this increase was mostly resulted from irreversible adsorption. Although, both air oxidized (AC2) and HNO_3 treated samples (AC3) had low tendencies to adsorb CO_2 irreversibly (<2% of total adsorption), 10-25% of total CO_2 adsorption was irreversible on Na_2CO_3 impregnated samples. From adsorption capacity loss after cycles, it can be concluded that Na_2CO_3 dispersion was higher on the HNO_3 treated samples than that on air oxidized samples. Additionally, CO_2 adsorption capacity after 2nd desorption shows that Na_2CO_3 impregnated air oxidized samples have higher adsorption capacity compared to Na_2CO_3 impregnated samples prepared on HNO_3 treated AC. This can be explained as follows: the dispersion was lower on air oxidized samples and after irreversible adsorption of CO_2 on Na_2CO_3 sites, there are still more vacant sites than that on the surface of the samples prepared on HNO_3 treated AC for CO_2 adsorption. High dispersion of Na_2CO_3 on HNO_3 treated samples can be explained with the high surface concentration of acidic oxygen bearing surface groups of AC3.

In overall, impregnation of Na_2CO_3 has increased the CO_2 adsorption capacity of all samples, however, after irreversible adsorption, reversible CO_2 uptake capacity of AC5a AC5b and AC5c is only ~3% grater than untreated AC1, in other words adsorption capacity loss of AC1 upon HNO_3 treatment was just reestablished upon Na_2CO_3 impregnation. Na_2CO_3 impregnated air oxidized samples AC4b and AC4c has also showed similar capacity with the unimpregnated air oxidized sample AC2 after 2nd adsorption cycle. Adsorption capacities of all related samples after 2nd cycle are showed in Figure 4.4.

Impregnation has also given rise to H_2 and CO adsorption on AC. As it can be followed from Table 4.6, unimpregnated samples AC0, AC1, AC2 and AC3 had less than 0.08 % adsorption capacity for H_2 and CO by weight, whereas, for impregnated samples this capacity was nearly 10 times more, ranging as high as 1.0%. However, due to the fact that, adsorption of H_2 and CO was less than 10% of adsorption of CO_2 in average and H_2

and CO showed irreversible adsorption characteristics (once exposed to H_2 and CO, adsorption capacities for this species were reduced to insignificant levels), it can still be concluded that CO_2 adsorption was selective on the samples after first adsorption cycle.

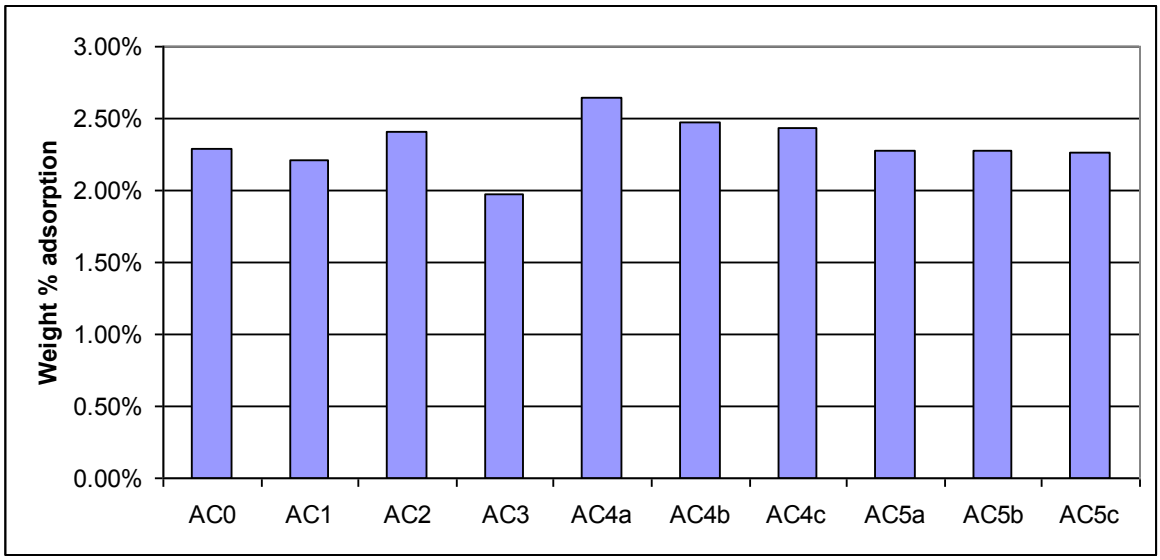

Figure 4.4 Weight % adsorption capacity after 2nd cycle

4.2.4. Effect of Calcination Temperature on CO_2 Adsorption

In the current study, no strong evidence was found that there was a relationship between calcination temperature and CO_2 adsorption capacity. However, Na_2CO_3 impregnated and 300 °C calcined sample (AC4a) prepared on air oxidized AC showed ~7% higher adsorption capacity with respect to samples which are calcined at 200 °C and 250 °C. Most probable reason for this increase is that the calcination at 300 °C resulted in decomposition most of the carboxylic groups as it can be seen from the TPD spectra in Figure A.3. Carboxylic groups are referred as the most acidic surface groups so the decrease in the amount of carboxyl groups might reduced the acidity of the surface, resulting in an increase in the reversible adsorption capacity. Effect of calcination temperature on reversible CO_2 adsorption on samples AC4a, AC4b, AC4c, AC5a, AC5b and AC5c is given in Figure 4.5.

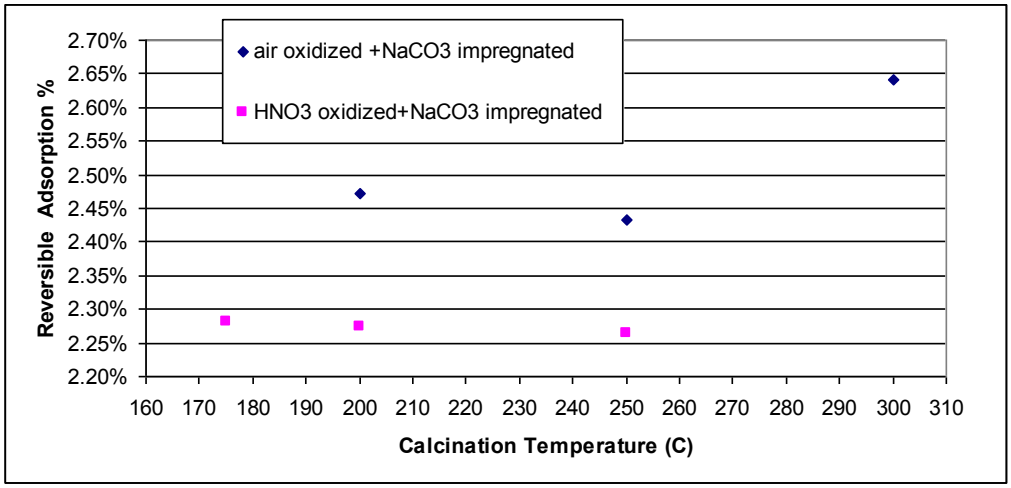

Figure 4.5 Effect of calcination temperature on air/HNO_3 oxidized and Na_2CO_3 impregnated ACs.

4.3. Butane Adsorption Studies under Static Conditions

Butane adsorption and desorption isotherms on samples AC10, AC11 and AC12 were obtained at 40 °C, 70 °C and 100 °C. Adsorption and desorption profiles of sample AC10 at 40 °C is given in Figure 4.6 as an example. It is easily seen that there is an exact match between adsorption and desorption profiles. This behavior is common for all three samples at the investigated temperatures.

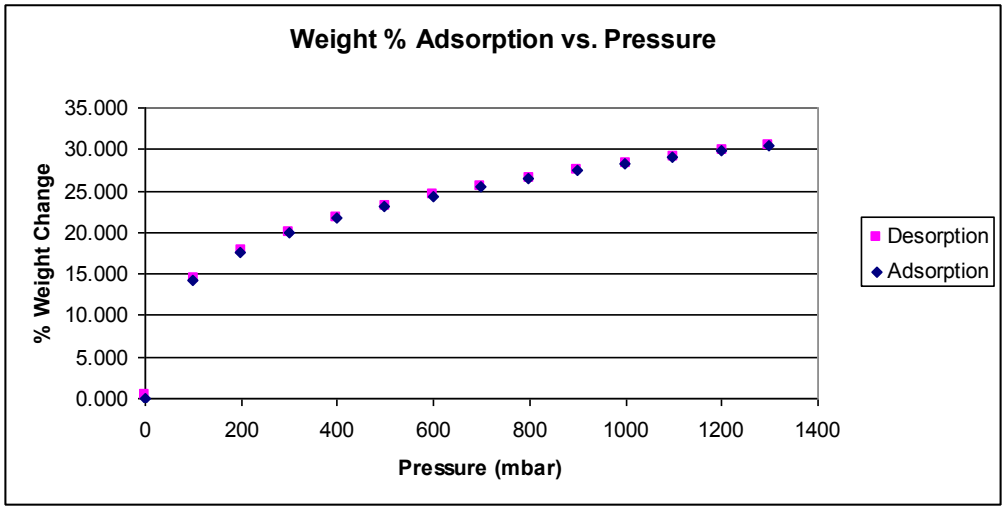

Figure 4.6. Butane adsorption and desorption profile of AC10 at 40 °C

Adsorption isotherms at 40 °C, 70 °C and 100 °C are given in Appendix B Figures B.1 – B.3 respectively. Weight per cent butane adsorption capacity of AC10, AC11 and AC12 at 1 bar is summarized in Figure 4.7.

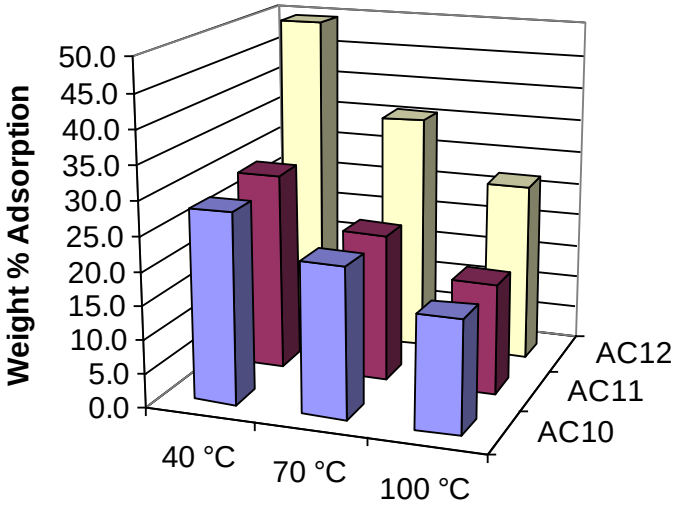

	40 °C	70 °C	100 °C
AC10	28.3	22.3	16.6
AC11	29.6	22.0	16.5
AC12	49.7	35.6	26.8

Figure 4.7 Butane adsorption capacities of AC10, AC11 and AC12 at 1 bar.

AC10 and AC11 have very similar adsorption capacities, ~29% by weight at 1 bar and 40 °C whereas, in the same conditions AC12 has much higher adsorption capacity, reaching as high as 50 % by weight.

4.3.1. Effect of Surface Area and Surface Chemistry on Butane Adsorption on AC

In order to study the relationship between surface area and adsorption capacity in detailed fashion, adsorption of butane per area were calculated via relation 4.7 and results were presented in Table 4.9 and Figure 4.8.

$$Adsorption\_Capacity\_per\_Area = \frac{Ads.Capacity}{BET\_surface\_area} \quad (4.7)$$

Table 4.9 Effect of surface area on butane adsorption capacity at 1bar

Sample	BET (m^2/g) m^2/g	40 °C Ads %	40 °C Ads/BET g butane /m^2	70 °C Ads %	70 °C Ads/BET g butane /m^2	100 °C Ads %	100 °C Ads/BET g butane /m^2
AC10	1147.2	28.29	0.0247	22.25	0.0194	16.58	0.0145
AC11	1100.9	29.56	0.0269	22.01	0.0200	16.51	0.0150
AC12	1773.8	49.67	0.0280	35.64	0.0201	26.81	0.0151

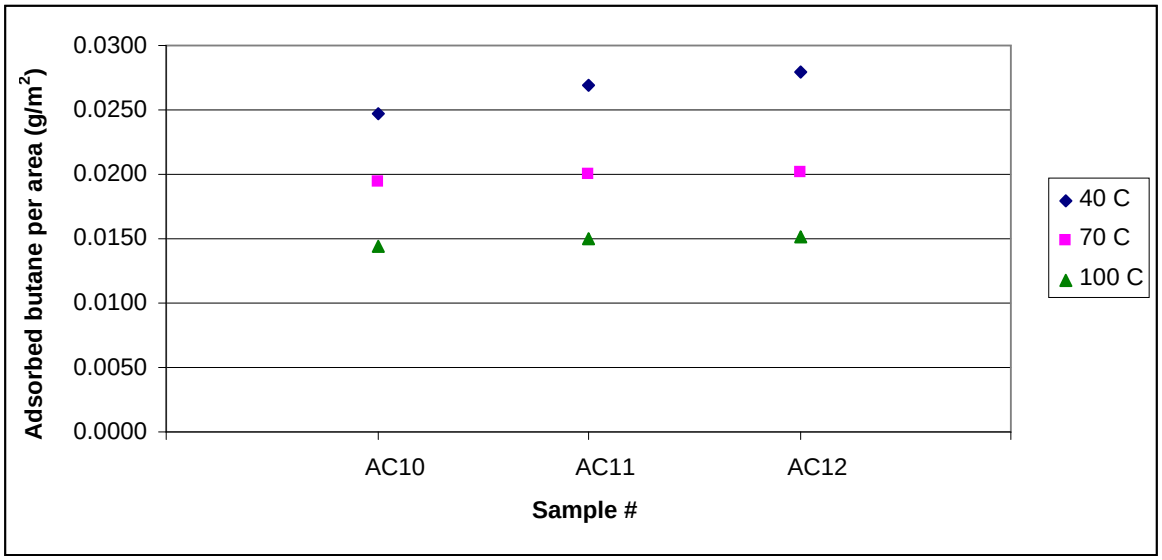

Figure 4.8 Adsorbed butane per area of AC10, AC11 and AC12 at 1 bar.

As it can be seen from Table 4.9 and Figure 4.8, there was a strong relationship between surface area and butane adsorption capacity. Adsorbed amount per area was very similar for all samples at each temperature however there was a discrepancy, which was small in magnitude, on the adsorption data at 40 °C. Although it is hard to conclude that this discrepancy was resulted from surface chemistry of AC, similar trend in the amount of carboxyl and anhydride groups are worth noting. In contrast upon inspection the amount of lactone, phenol and carbonyl/quinone on the surface of AC10, AC11 and AC12, it can be concluded that contribution of these groups on the adsorption capacity is rather small or

insignificant. Against its adsorption capacity; AC11 has the largest amount of lactones and carbonyl/quinone, whereas AC12 is the one which has the least amount of these groups. Additionally the amount of phenol is significantly different between AC10 and AC11, which in return has very negligible effect on the butane adsorption.

In general evaluation, surface area of the samples is a far more determining factor in butane adsorption capacity on AC10, AC11 and AC12 samples.

4.3.2. Cyclic Adsorption Capacity in Static Butane Adsorption Tests

Samples AC10, AC11 and AC12 showed excellent cyclic adsorption ability on pure butane. Cyclic behavior was investigated in 10 cycles as explained in section 3.2.1. Equilibrium weights at 1 bar in each cycle are given for AC10, AC11 and AC12 in Figures 4.9-4.11 respectively. Adsorption loss was less than 1% between cycles, which proves that butane adsorption on activated carbon was fully reversible.

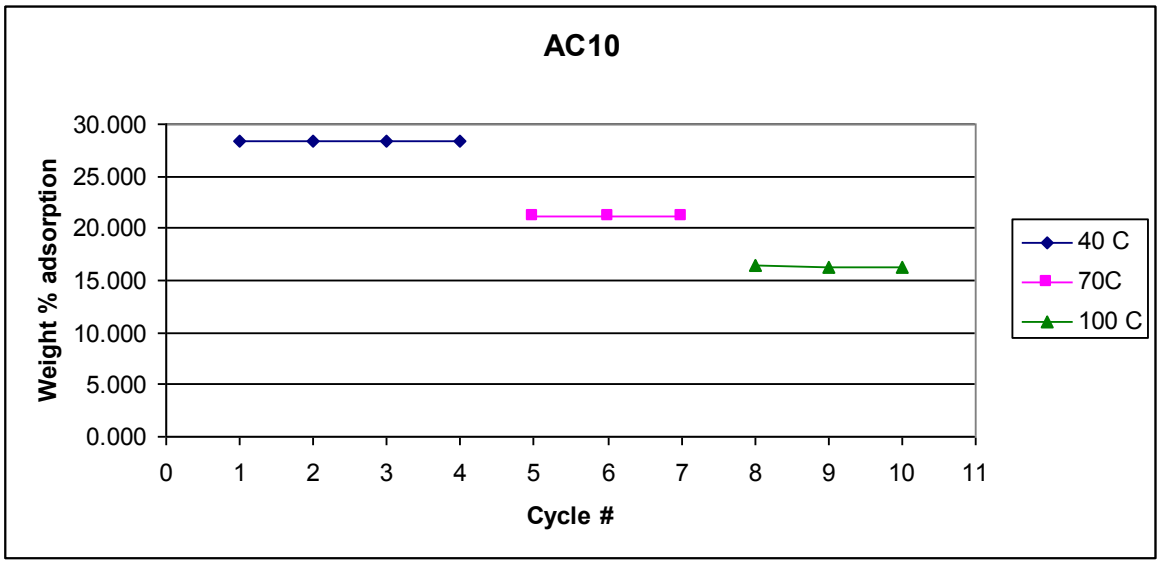

Figure 4.9 Cyclic adsorbed weight % at 1 bar (AC10)

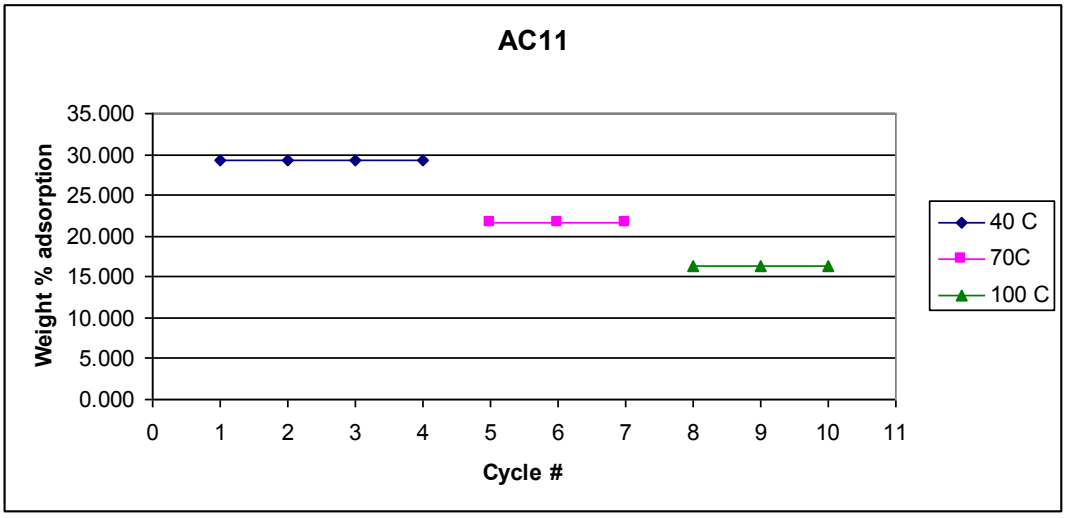

Figure 4.10 Cyclic adsorbed weight % at 1 bar (AC11)

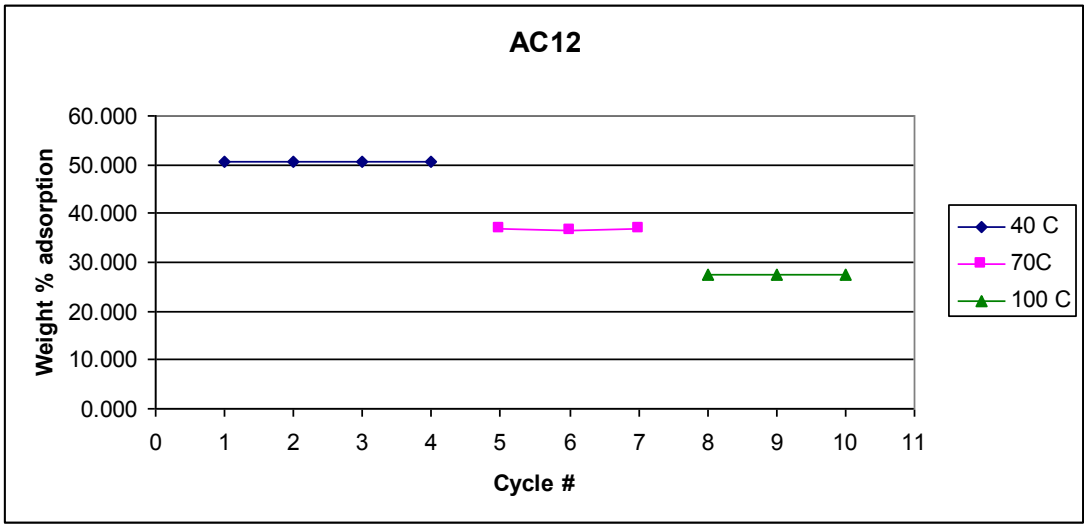

Figure 4.11 Cyclic adsorbed weight % at 1 bar (AC12)

4.3.3. Langmuir Fit and ΔH of Butane Adsorption

Adsorption data were fitted to linearized form of Langmuir equation; from the straight line fit on the graph of P/V vs P, Langmuir constants Vm and b were obtained. Langmuir fit to butane adsorption data of AC10 at 40 °C is given as an example in Figure 4.12.

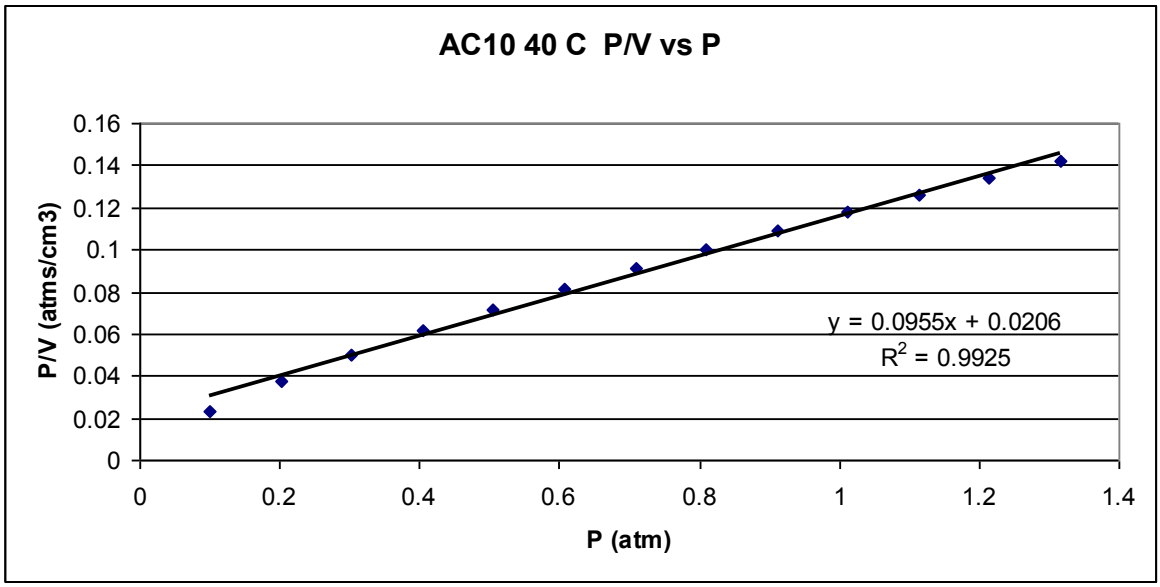

Figure 4.12 Straight line fit on P/V vs P plot in order to determine Langmuir constants

Table 4.10 Langmuir constants and R^2

Sample	T (°C)	Vm (cm^3)	b (1/atm)	R^2
AC10	40	10.471	4.63	0.993
	70	8.271	4.08	0.994
	100	6.515	3.28	0.993
AC11	40	11.173	4.16	0.991
	70	8.511	3.75	0.993
	100	7.231	2.95	0.993
AC12	40	19.157	3.76	0.989
	70	13.986	3.42	0.992
	100	9.804	2.63	0.992

High R^2 values in the last column of Table 4.10 shows that butane adsorption on activated carbon can be represented by Langmuir isotherm; thus it is possible to calculate heat of adsorption from following relation, which is derived from Classius Clapeyron equation:

$$\langle Vm \cdot b \rangle = A_c \exp\left(\frac{-\Delta H}{R \cdot T}\right) \tag{4.8}$$

where A_c is a constant containing the entropy term, R is the universal gas constant and ΔH is the enthalpy of adsorption. ΔH/R. can be obtained by taking the negative of the slop of the straight line fitted to $Ln(V_m \cdot b)$ vs. $1/T$ plot (Farah *et al*., 2007). Straight line fits to $Ln(V_m \cdot b)$ vs. $1/T$ plots and calculated heat of adsorption data are given in Figure 4.13 and Table 4.11 respectively.

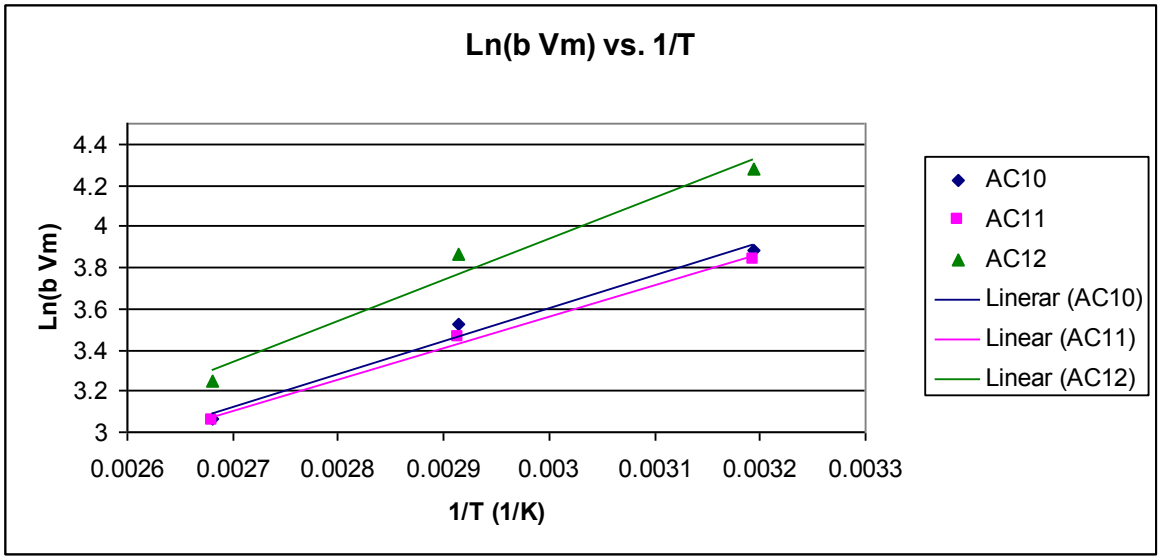

Figure 4.13 Straight line fit to $Ln(V_m \cdot b)$ vs. $1/T$ plot

Table 4.11 ΔH of adsorption and success of the fit of equation 4.8

Sample	R^2	Heat of adsorption (kj/mol)
AC10	0.986	-13.2
AC11	0.995	-12.6
AC12	0.972	-16.5

Table 4.11 and Figure 4.13 show a good correlation between the adsorption data and Langmuir isotherms. Expectedly AC10 and AC11 has similar heat of adsorption values whereas AC12 has lower heat of adsorption showing a higher tendency to adsorb butane molecules compared to those of AC10 and AC11.

5. CONCLUSIONS AND RECOMMENDATIONS

5.1. Conclusions

5.1.1. Selective CO_2 Adsorption Studies in Dynamic Conditions

The effect of oxidation methods on textural and surface chemical properties of commercial Norit ROX based activated carbon was investigated. Changes in the CO_2 adsorption capacity, in response to Na_2CO_3 impregnation and calcination temperature on the adsorption behavior was discussed. The result revealed that:

- HCl washing increased the amounts of surface groups especially phenols significantly whereas a reduction was observed in anhydride and carboxyl groups after HCl washing.
- Air oxidation resulted in an increase in anhydrides and carbonyl quinones whereas amount of lactones and carboxyls were reduced in limited amounts. In addition, 20% increase in the BET surface area with air oxidation was reported previously.
- HNO_3 oxidation has very strong influence on surface chemistry of activated carbons. Carboxylic, anhydridic, lactonic and phenolic surface groups has increased significantly, whereas reported surface area was 7% less than unoxidized sample.

HCl washing and oxidation treatments have affected the selective CO_2 adsorption behavior of AC samples in the following ways:

- HCl washing has decreased reversible CO_2 adsorption ability of AC0 by 4%
- Air oxidation resulted in a 9% increase in the CO_2 adsorption capacity.
- Adsorption capacity was reduced 10.8% upon HNO_3 oxidation. This decrease can be a result of both 7% decrease in total surface area and significant increase in the amount of acidic surface groups, namely carboxyls, lactones and phenols, which may result in the repulsion of CO_2 molecules.

Effects of Na_2CO_3 impregnation and calcination of AC samples on CO_2 adsorption are summarized below:

- Na_2CO_3 impregnation has increased CO_2 adsorption capacity of all samples significantly whereas this increase was mostly resulted form irreversible adsorption. Nearly 10% of the total CO_2 adsorption was irreversible on the air oxidized and Na_2CO_3 impregnated samples whereas, irreversible adsorption was found as high as 25% of total CO_2 adsorption for samples prepared by Na_2CO_3 impregnation on HNO_3 oxidized AC.
- Higher irreversible CO_2 adsorption on AC5a, AC5b, and AC5c pointed out higher dispersion of Na_2CO_3 on the HNO_3 oxidized AC compared to that on the air oxidized AC. Increase in the acidic surface groups upon HNO_3 oxidation may be a strong reason on the high dispersion of Na_2CO_3.
- Reversible CO_2 adsorption capacity has increased with Na_2CO_3 impregnation. Capacity loss with oxidation has been reversed for NHO_3 oxidized samples. Whereas, however small in magnitude, capacity was further increased with impregnation on the air oxidized sample.
- Na_2CO_3 impregnation has also increased the H_2 and CO adsorption on the AC. Unimpregnated samples have nearly no tendency to adsorb H_2 and CO whereas impregnated samples adsorbed H_2 and CO up to 1% by weight. However adsorption of H_2 and CO is irreversible thus has no effect on the CO_2 adsorption selectivity.
- No significant relationship between calcination temperature and dynamic CO_2 adoption capacity was observed on the samples AC4a, AC4b, AC4c, AC5a, AC5b, and AC5c which are calcined after Na_2CO_3 impregnation at 300 °C, 200 °C, 250 °C, 175 °C, 200°C and 250 °C respectively. However AC4a, which is calcined at 300 °C, have shown higher adsorption capacity with respect to other samples. Possible reason for increase in capacity is that calcination may result in the removal of some of the carboxylic groups which are considered as the most acidic oxygen bearing surface groups on the surface of AC.

5.1.2. Butane Adsorption Studies under Static Conditions

Another purpose of the current study was to investigate butane adsorption capacity of commercial AC samples (AC10, AC11 and AC12), which were provided by Ford Otosan A. Ş. The Results obtained are summarized below:

- All of the AC samples showed good adsorption characteristics. Adsorption and desorption curves coincide exactly. Butane adsorption capacity of samples AC10, AC11 and AC12 was 28.3%, 29.6% and 49.7% by weight at 1 bar and 40 °C respectively.
- There was a strong relationship between BET surface area and butane adsorption capacity at 1bar. However, there was a small discrepancy between surface area and adsorption capacity at 40 °C. Although it is hard to conclude that this discrepancy is a result of the surface chemistry diversity, similar trend has been seen in the amount of carboxyl and anhydride surface groups and the adsorption capacity at 40 °C. Contributions of lactone, phenol and carbonyl/quinone groups on the adsorption capacity were found insignificant.
- AC10, AC11 and AC12 showed excellent cyclic behavior for butane adsorption. Less than 1% adsorption loss was observed after 10 adsorption/desorption cycles.
- Langmuir fit on the adsorption data showed excellent correlation proving adsorption can be represented with Langmuir isotherm. Heat of adsorption was found as -13.2 kj/mol, -12.6 kj/mol and -16.5 kj/mol for samples AC10, AC11 and AC12, respectively, through using modified form of Clasius Clapeyron relation by utulizing Langmuir parameters obtained.

5.2. Recommendations

There exists a need for further investigation to fully characterize AC samples. Fitting of DR equation on adsorption data for CO_2 adsorption in low relative pressures at 0 °C and N_2 adsorption data at 77 K can reveal micro and meso porosity of AC. Additionally, as the related literature states that basic nitrogen functionalities have strong influence on the CO_2,

determination of nitrogen bearing surface groups via TPSGD analysis may have a strong contribution to a similar study.

In addition, CO_2 adsorption tests should be conducted on calcined samples (without Na_2CO_3 impregnation) to fully comprehend the effect of calcination on the selective CO_2 adsorption behavior.

APPENDIX A: TPD DECONVOLUTION SPECTRA

Oxygen bearing surface groups of samples AC0, AC1, AC2, AC3, AC10, AC11 and AC12 were obtained by deconvolution of TPD spectra to Gaussian peaks by using a Matlab program written by Assoc. Prof. Hasan Bedir. Program utilizes non linear optimization sequence in order to reduce the discrepancy between CO/CO2 decomposition and the sum of the generated Gaussian peaks. Initial guess for peak temperatures for surface groups, as well as upper and lower temperature limits were set according to previously obtained parameters in the literature (Aksoylu *et al.*, 1999; Figueiredo *et al.*, 1999). Results of the deconvolutions are summarized in Figures A.1-A.7.

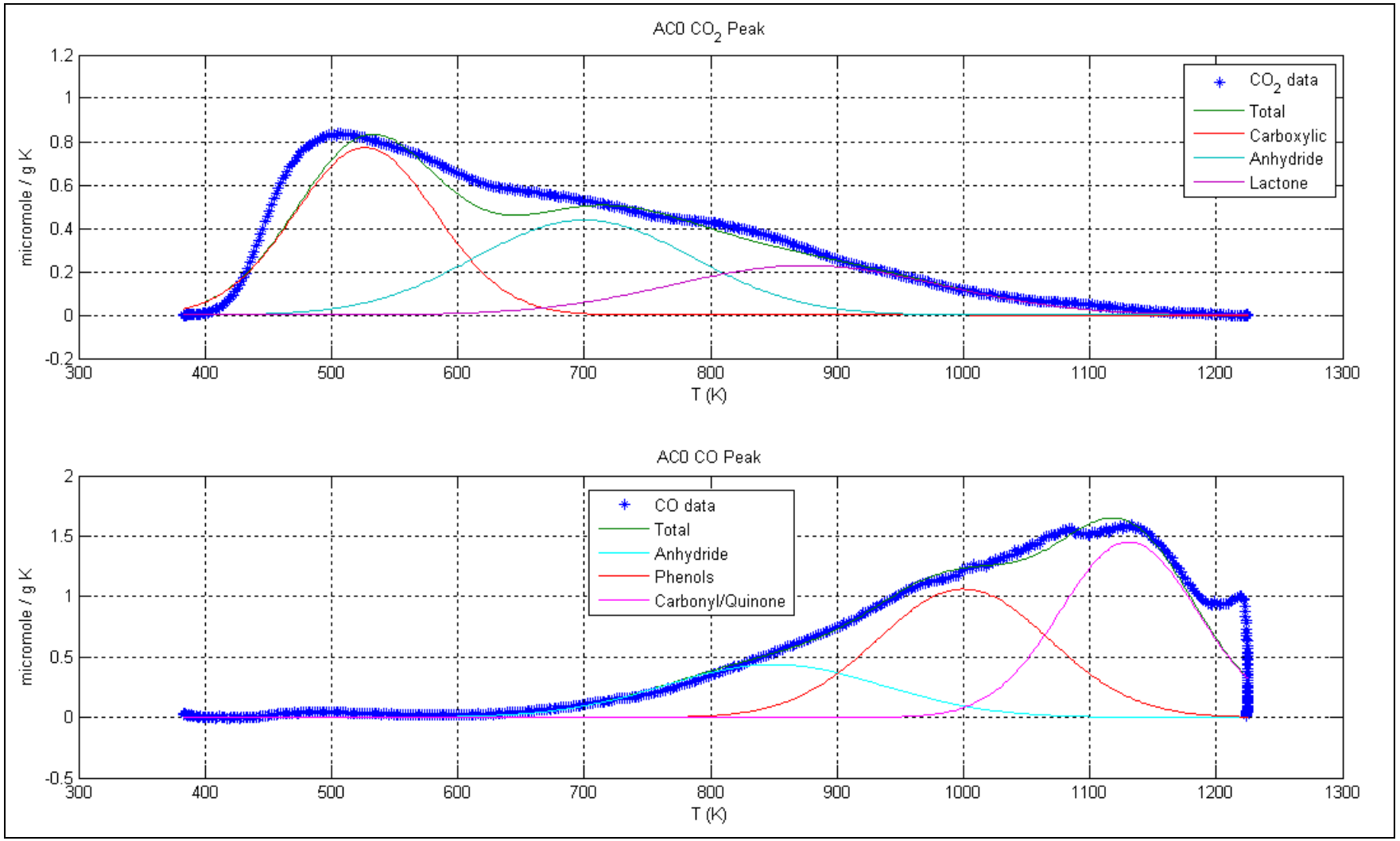

Figure A.1 TPD deconvolution of AC0

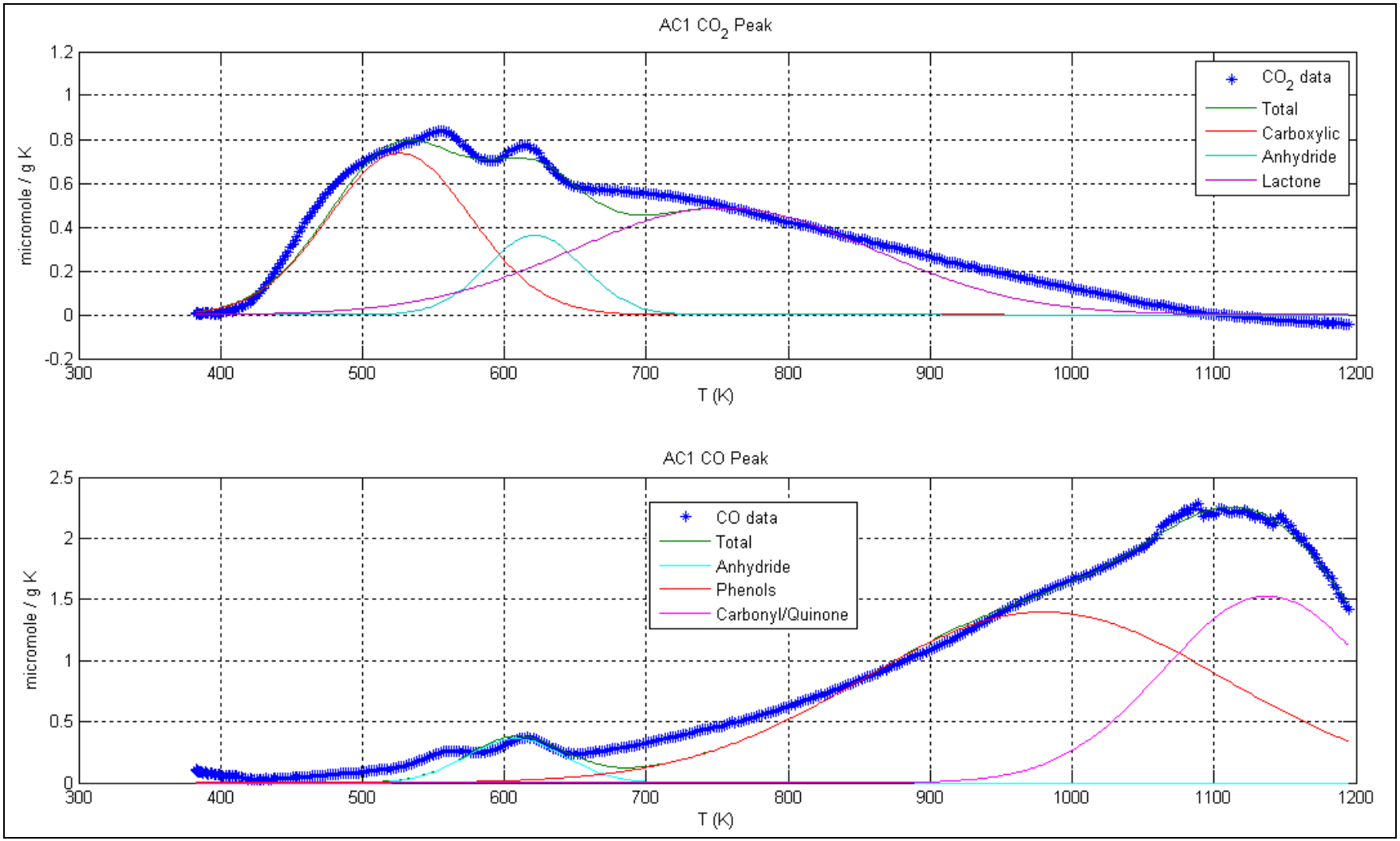

Figure A.2 TPD deconvolution of AC1

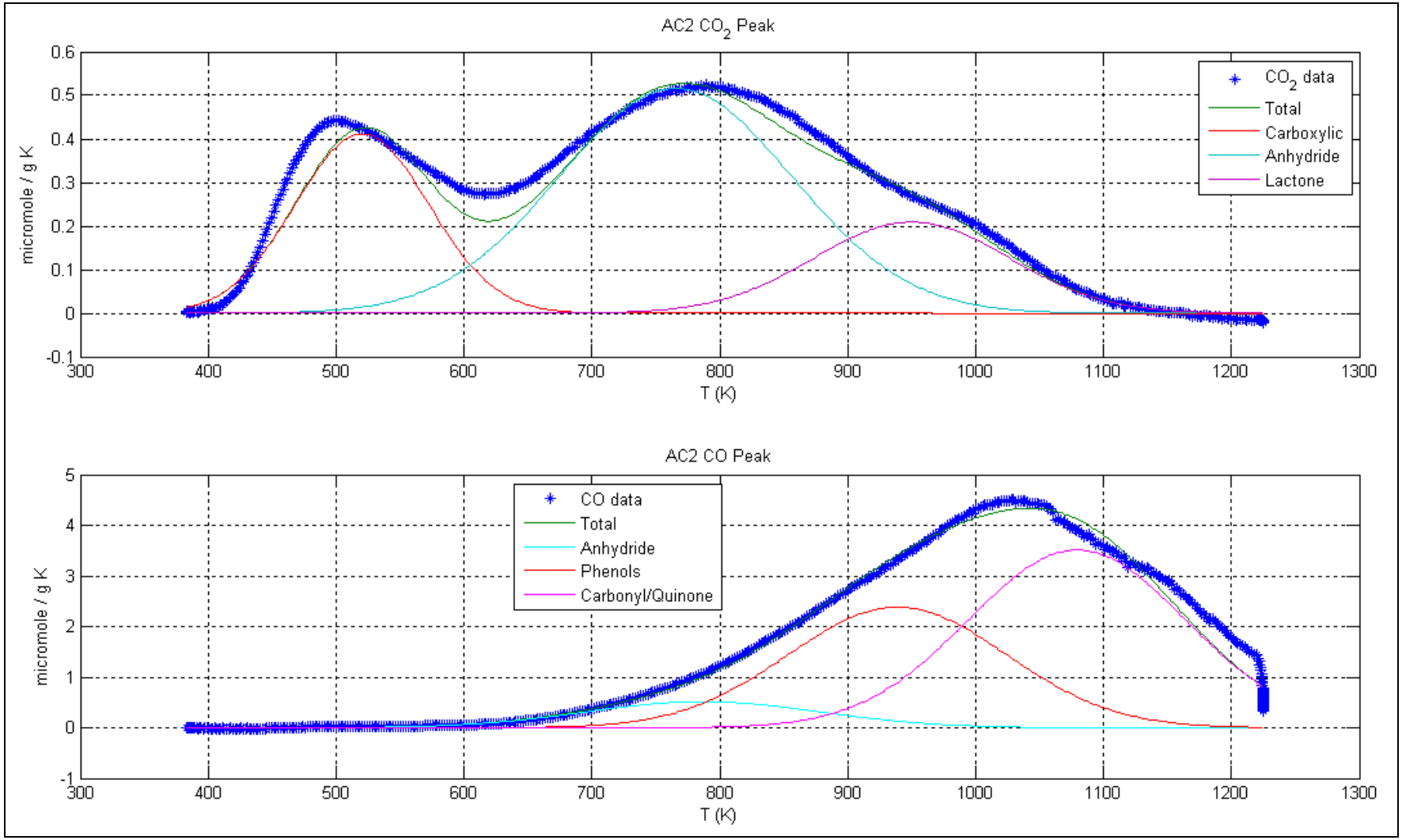

Figure A.3 TPD deconvolution of AC2

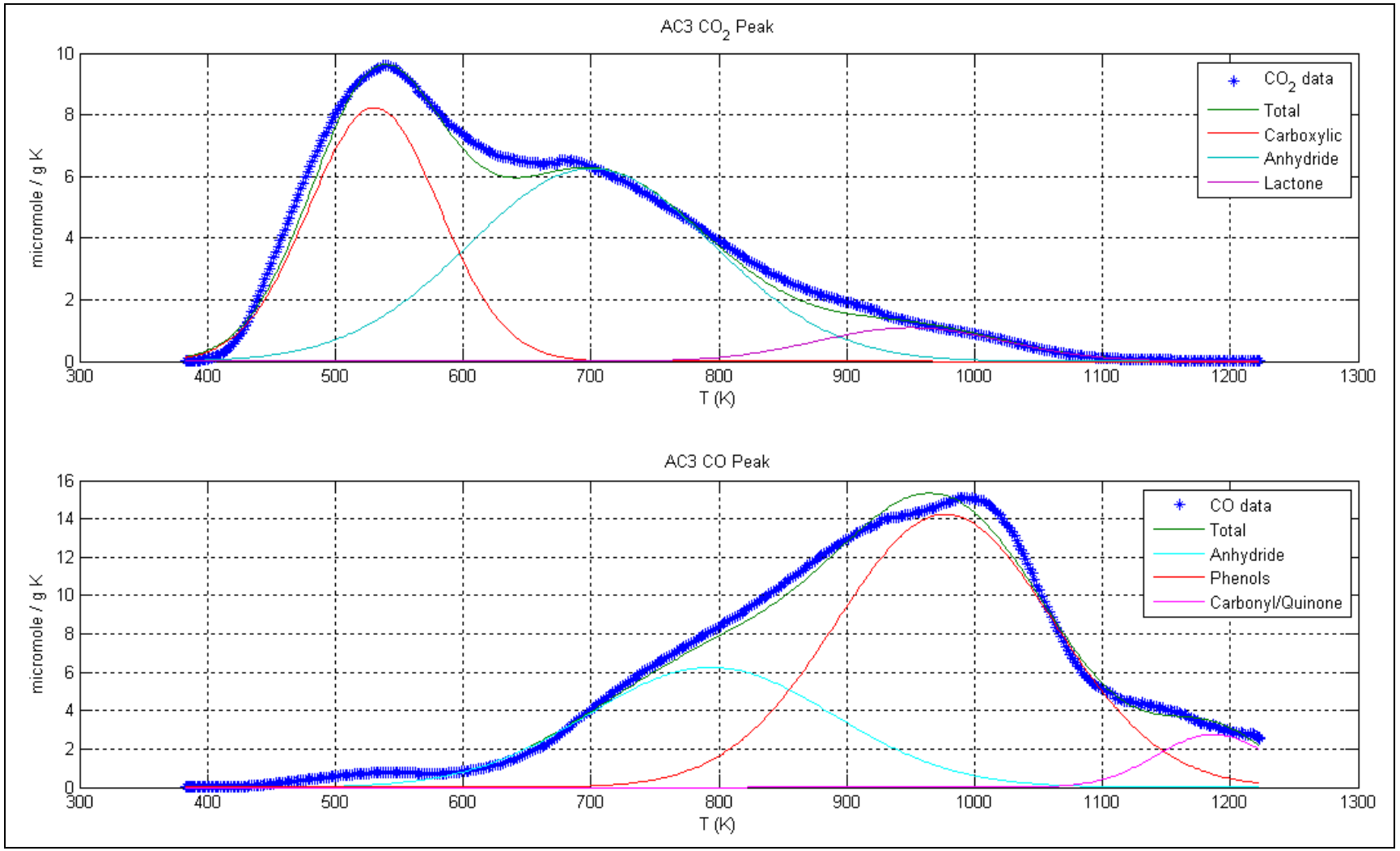

Figure A.4 TPD deconvolution of AC3

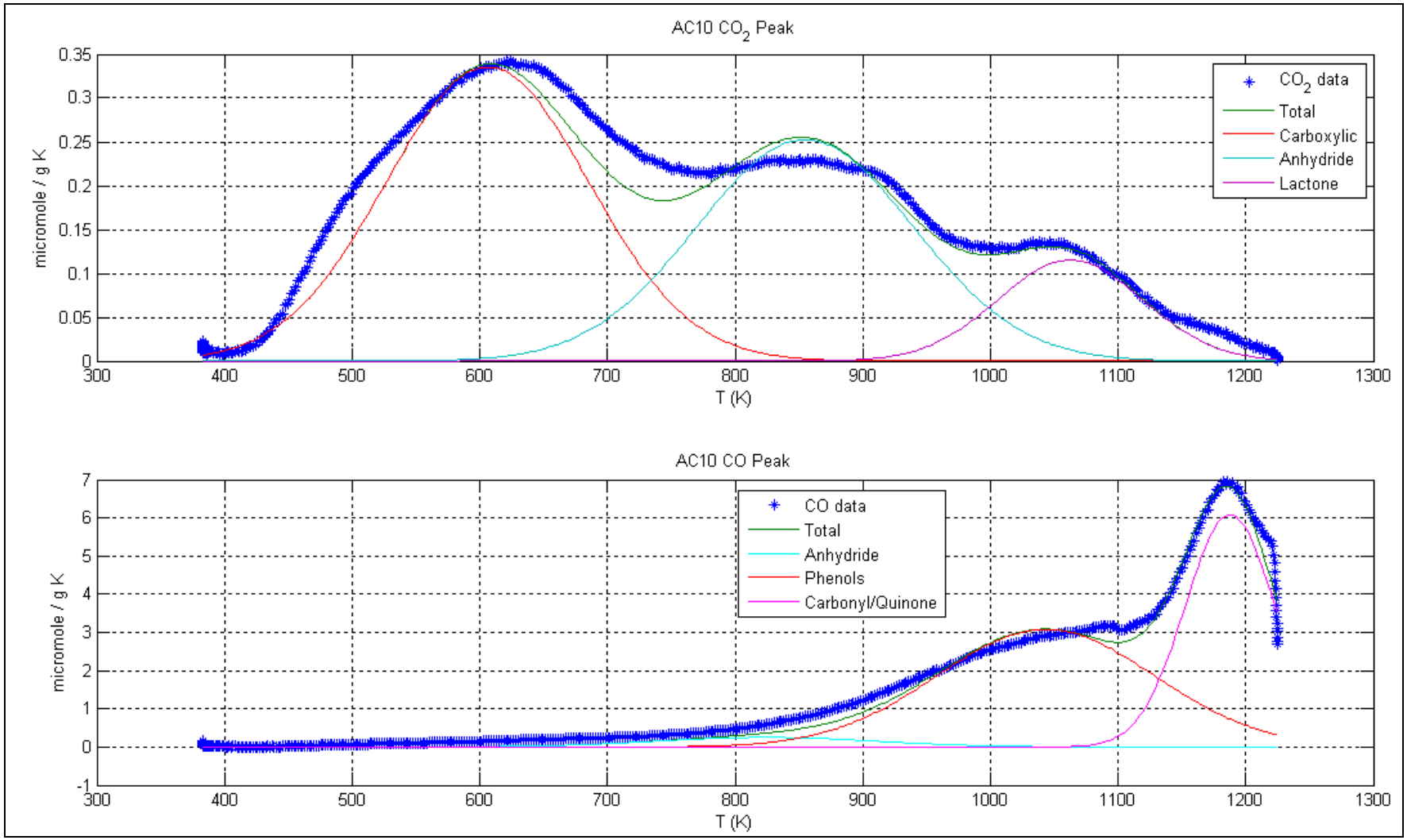

Figure A.5 TPD deconvolution of AC10

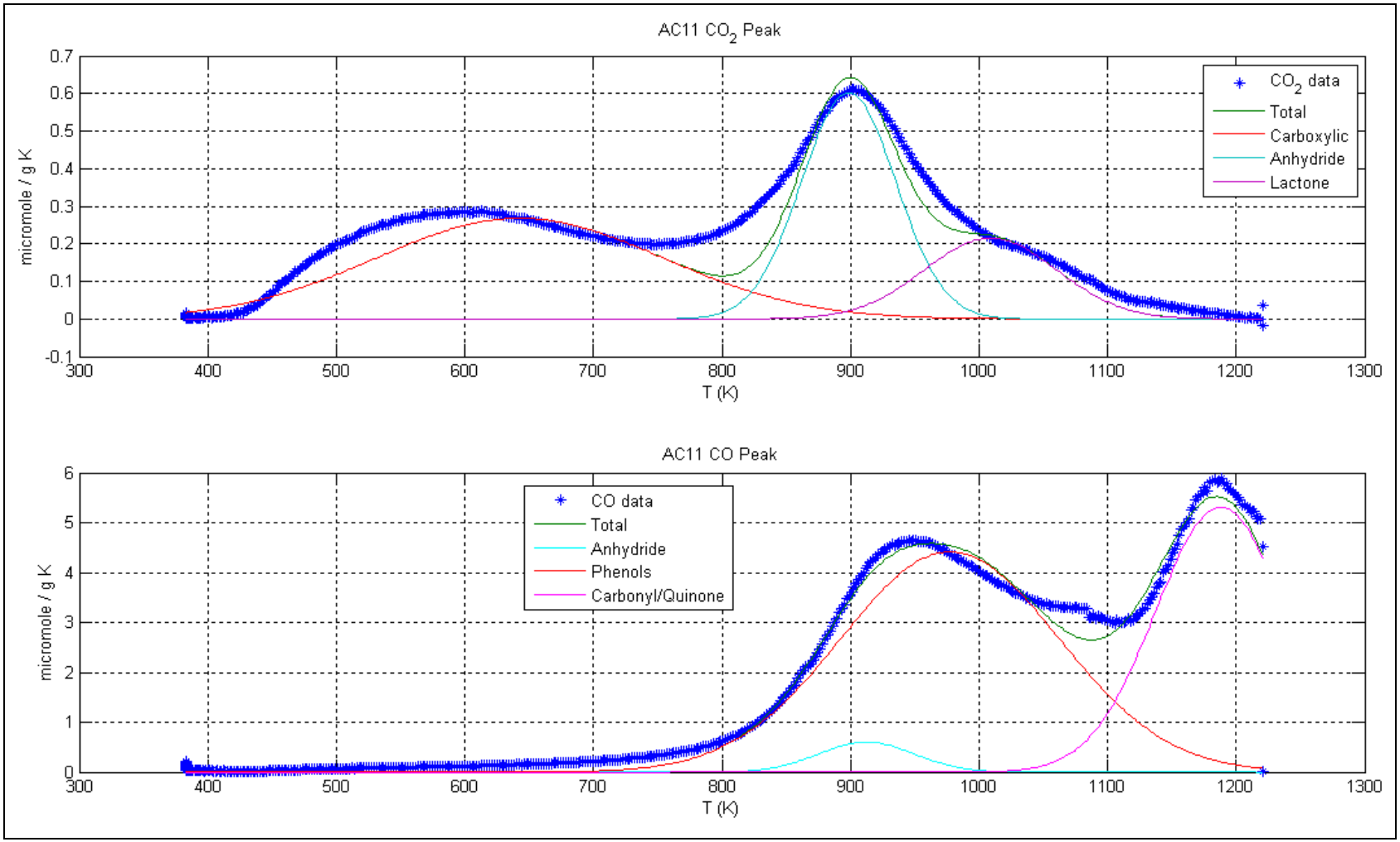

Figure A.6 TPD deconvolution of AC11

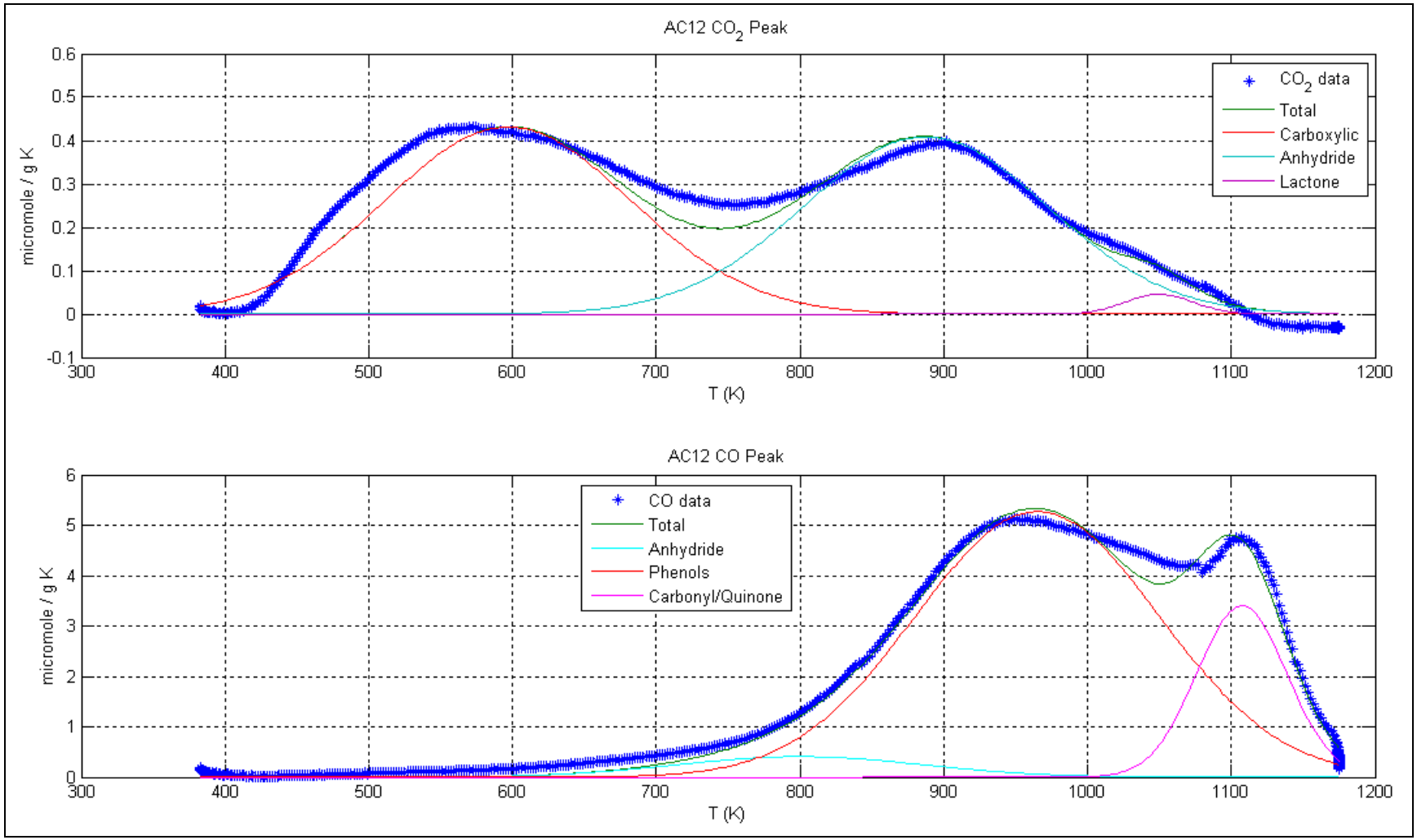

Figure A.7 TPD deconvolution of AC12

APPENDIX B: BUTANE ADSORPTION DATA

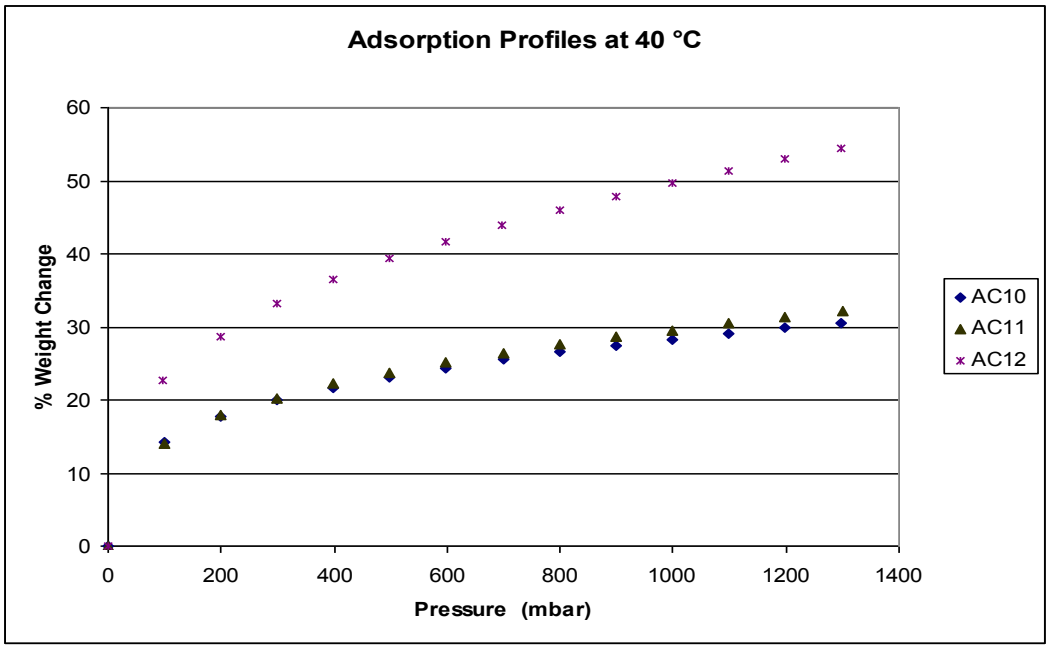

Figure B.1 Butane adsorption isotherms at 40 °C

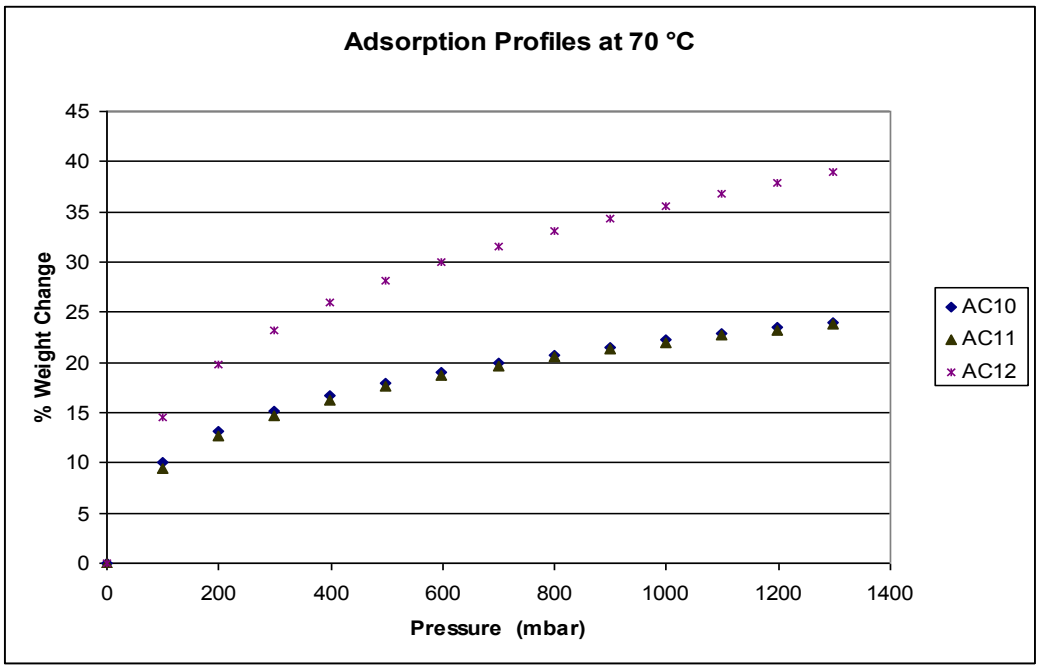

Figure B.2 Butane adsorption isotherms at 70 °C

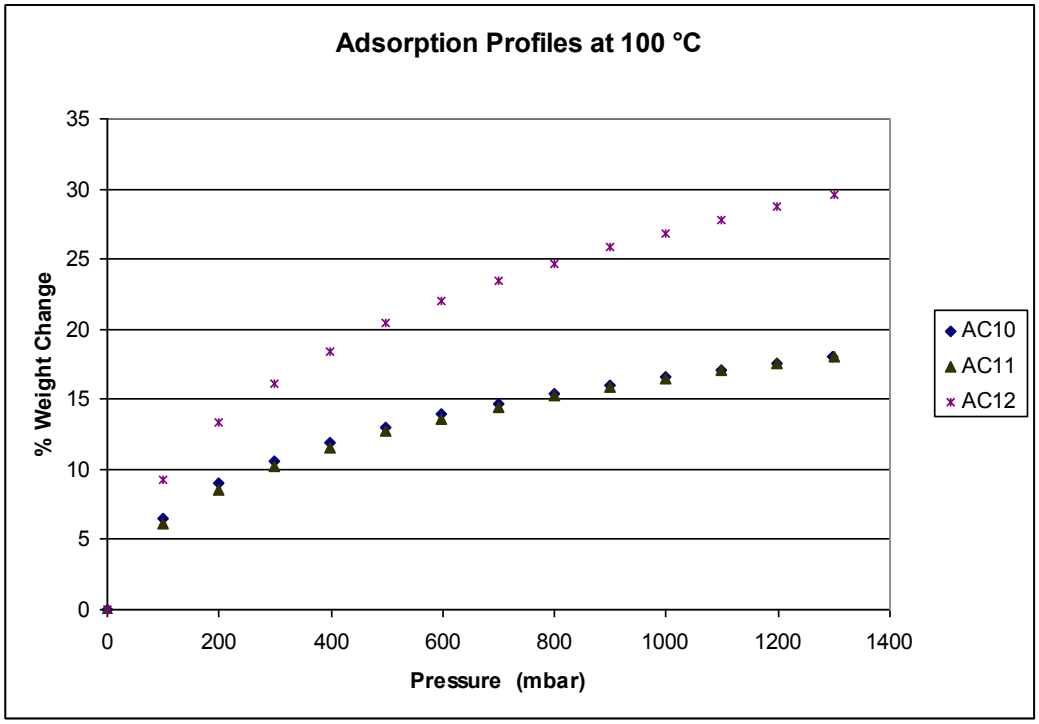

Figure B.3 Butane adsorption isotherms at 100 °C

REFERENCES

Aksoylu A. E., M. Madalena, A. Freitas, J. L. Figueiredo, 2000, "Bimetallic Pt–Sn Catalysts Supported on Activated Carbon: I. The Effects of Support Modification and Impregnation Strategy", *Applied Catalysis A: General*, Vol. 192, pp. 29–42.

Aksoylu A. E., M. Madalena, A. Freitas, M. Fernando, R. Pereira, J. L. Figueiredo, 2001, "The Effects of Different Activated Carbon Supports and Support Modifications on the Properties of Pt/AC Catalysts", *Carbon*, Vol. 39, pp. 175–185.

Auer E., E. Freund, J. Pietsch, T. Tacke, 1998, "Carbons as Supports for Industrial Precious Metal Catalysts", *Applied Catalysis A*, Vol. 173, pp. 259-271.

Bansal R. C. and M. Goyal, *Activated Carbon Adsorption*, CRC Press, Boca Raton, 2005.

Boehm, H.P., 1966, "Chemical Identification of Surface Groups", *Advances in Catalysis*, Vol. XVI, Academic Press, New York, pp. 179.

Bruijn F.A., D. C. Papageorgopoulos, E. F. Sitters, G. J. M. Janssen, 2002, "The Influence of Carbon Dioxide on PEM Fuel Cell Anodes", *Journal of Power Sources*, Vol. 110, pp. 117–124.

Brunauer S., H. Emmet, E. Teller, 1938, "Adsorption of Gases in Multimolecular Layers", *Journal of American Chemical Society*, Vol. 60, pp.309.

Chlendi M. and D. Tondeur, 1995, "Dynamic Behavior of Layered Columns in Pressure Swing Adsorption", *Gas Separation & Purification*, Vol. 9, pp. 231-242.

Dias J. M., M. C. M. Alvim-Ferraz, M. F. Almeida, J. Rivera-Utrilla, M. Sanchez-Polo, 2007, "Waste Materials for Activated Carbon Preparation and Its Use in Aqueous-

Phase Treatment: A Review", *Journal of Environmental Management*, Vol. 85, pp. 833–846.

Diaz E., S. Ordonez, A. Vega, J. Coca, 2004, "Adsorption Characterization of Different Volatile Organic Compounds Over Alumina, Zeolites and Activated Carbon Using Inverse Gas Chromatography", *Journal of Chromatography A*, Vol. 1049, pp. 139–146.

Dubinin, M.M. and D.P. Timofeev, 1946, "Adsorption of vapors on active carbons in relation to the properties of the adsorbate", *Doklady Akademii Nauk SSSR*, Vol. 54, pp. 701–704.

European Commission 1998. "Directive 98/69/EC of the European Parliament and of the Council relating to measures to be taken against air pollution by emissions from motor vehicles and amending Council Directive 70/220/EEC." *Official Journal of the European Communities*, L 350, 28.12.98, pp. 31.

Farah J. Y., N. S. El-Gendy, L. A. Farahat, 2007, "Biosorption of Astrazone Blue Basic Dye from an Aqueous Solution Using Dried Biomass of Baker's yeast", *Journal of Hazardous Materials*, Vol. 148, pp. 402–408.

Figueiredo J. L., M. F. R. Pereira, M. M. A. Freitas, J. J. M. Orfao, 1999, "Modification of the Surface Chemistry of Activated Carbons", *Carbon*, Vol. 37, pp. 1379–1389.

Gürdağ S., 2001, *An Investigation on the Use of Activated Carbon Supported Noble Metal Catalysts in CO Oxidation*, M.S. Thesis, Boğaziçi University.

Hutson N. D., R. T. Yang, 1997, "Theoretical Basis for the Dubinin-Radushkevitch (D-R) Adsorption Isotherm Equation", *Adsorption*, Vol. 3, pp. 189-195.

IUPAC, 1972, "Manual of Symbols and Terminology, Appendix 2, Part I, Colloid and surface Chemistry", *Pure and Applied Chemistry*, Vol.31, pp. 578.

Karatepe N., İ. Orbak, R. Yavuz, A. Özyoğuran, 2008, "Sulfur Dioxide Adsorption by Activated Carbons Having Different Textural and Chemical Properties", *Fuel*, Vol. 87, pp. 3207–3215.

Langmuir, I., 1918, *Journal of American Chemical Society*, Vol. 40, pp. 1361.

Majlan E. H., W. R. W. Daud, S. E. Iyukeb, A. B. Mohamad, A. A. H. Kadhum, A. W. Mohammad, M. S. Takriff, N. Bahaman, 2009, "Hydrogen Purification Using Compact Pressure Swing Adsorption System for Fuel Cell", *International Journal of Hydrogen Energy*, Vol. 34, pp. 2771-2777.

Marsh H. and F. Rodriguez-Reinoso, 2006, *Activated Carbon*, Elsevier Science & Technology Books.

Marchon B., J. Carrazza, H. Heinemann, G. A. Somorjai, 1988, "TPD and XPS Studies of O_2, CO_2, and H_2O Adsorption on Clean Polycrystalline Graphite", *Carbon*, Vol. 26, pp. 507.

Mangun C. L., M. A. Daley, R. D. Braatz, J. Economy, 1998, "Effect of Pore Size on Adsorption of the Hydrocarbons in Phenolic-Based Activated Carbon Fibers", *Carbon*, Vol. 36, pp. 123-131.

Mellios G. and Z. Samaras, 2007, "An Empirical Model for Estimating Evaporative Hydrocarbon Emissions from Canister-Equipped Vehicles", *Fuel*, Vol. 86, pp. 2254–2261.

Moreno-Castilla C., M. V. Lopez-Ramon, F. Carrasco-Marın, 2000, "Changes in Surface Chemistry of Activated Carbons by Wet Oxidation", *Carbon*, Vol. 38, pp. 1995–2001.

Moreno-Castilla C. and J. Rivera-Utrilla, 2001, "Carbon Materials as Adsorbents for the Removal of Pollutants from the Aqueous Phase", *Materials Research Society Bulletin*, Vol. 26, pp. 890–894.

Otake Y. and R. G. Jenkins, 1993, "Characterization of Oxygen-Containing Surface Complexes Created on a Microporous Carbon by Air and Nitric Acid Treatment", *Carbon*, Vol. 31, pp. 109-121.

Pellerano M., P. Pascaline, M. Kacem, A. Delebarre, 2009, "CO_2 Capture by Adsorption on Activated Carbons Using Pressure Modulation", *Energy Procedia*, Vol. 1, pp. 647–653.

Pereira M. F. R., J. J. M. Órfão, J. L. Figueiredo, 2004, "Influence of the Textural Properties of an Activated Carbon Catalyst on the Oxidative Dehydrogenation of Ethylbenzene", *Colloids and Surfaces A*, Vol. 241, pp. 165–171.

Plaza M.G., C. Pevida, B. Arias, J. Fermoso, F. Rubiera, J. J. Pis, 2009, "A Comparison of Two Methods for Producing CO_2 Capture Adsorbents", *Energy Procedia*, Vol. 1, pp.1107–1113.

Plaza M.G., Pevida C., Arias B., Fermoso J., Casal M. D., Martin C. F., Rubiera F., Pis J.J., 2009, "Development of Low-Cost Biomass-Based Adsorbents for Postcombustion CO_2 Capture", *Fuel* (Article in Press).

Rodriguez-Reinoso F., 1998, "The Role of Carbon Materials in Heterogeneous Catalysis", *Carbon*, Vol. 36, pp. 159-175.

Rodriguez-Reinoso F. and M. Molina-Sabio, 1998, "Textural and Chemical Characterization of Microporous Carbons" *Advances in Colloid and Interface Science*, Vol. 76-77, pp.276-294.

Rodríguez-Reinoso F., J. Garridoa, J. M. Martín-Martíneza, M. Molina-Sabio, R. Torregrosa, 1989, "The Combined Use of Different Approaches in the Characterization of Microporous Carbons", *Carbon*, Vol. 27, pp. 23-32.

Saha B. B., A. Chakraborty, S. Koyama, S. Yoon, I. Mochida, M. Kumja, C. Yap, K. C. Ng, 2008, "Isotherms and Thermodynamics for the Adsorption of N-butane on Pitch Based Activated Carbon", *International Journal of Heat and Mass Transfer*, Vol. 51, pp.1582–1589.

Silvestre-Albero A., J. Silvestre-Albero, A. Sepúlveda-Escribanoa, F. Rodríguez-Reinoso, 2009, "Ethanol Removal Using Activated Carbon: Effect of Porous Structure and Surface Chemistry", *Microporous and Mesoporous Materials*, Vol. 120, pp. 62-68.

Somy A., M. R. Mehrnia, H. D. Amrei, A. Ghanizadeh, Safari M., 2009, "Adsorption of Carbon Dioxide Using Impregnated Activated Carbon Promoted by Zinc", *International Journal of Greenhouse Gas Control*, Vol. 3, pp. 249-254.

Soykal İ. I., 2008, *Preferential Oxidation Performace of Pt-Sn/AC Catalysts*, M.S. Thesis, Boğaziçi University.

Studbaker M. L., E. W. D. Huffman, A. C. Wolfe, L. G. Nabors, 1956, "Oxygen Containing Group on the Surface of Carbon Black", *Industrial and Engineering Chemistry*, Vol. 48, pp. 162-166.

Sumathi S., S. Bhatia, K. T. Lee, A. R. Mohamed, 2009, "Performance of an Activated Carbon Made from Waste Palm Shell in Simultaneous Adsorption of SOx and NOx of Flue Gas at Low Temperature" *Science in China Series E: Technological Sciences* (Article in press).

Quinlivan Li. L., P. A. Knappe, 2002. "Effects of Activated Carbon Surface Chemistry and Pore Structure on the Adsorption of Organic Contaminants from Aqueous Solution", *Carbon*, Vol.40, pp. 2085–2100.

Xue Y., Y. Guo, Z. Zhang, Y. Guo, Y. Wang, G. Lu, 2008, "The Role of Surface Properties of Activated Carbon in the Catalytic Reduction of NO by Carbon", *Applied Surface Science*, Vol. 255, pp. 2591–2595.

Yan R., D. T. Liang, L. Tsen, Y. P. Wong, Y. K. Lee, 2005, "Bench-Scale Experimental Evaluation of Carbon Performance on Mercury Vapour Adsorption", *Fuel*, Vol. 83, pp. 2401–2409.

Yang H., Z. Xua, M. Fan, A. E. Bland, R. R. Judkins, 2007, "Adsorbents for Capturing Mercury in Coal-Fired Boiler Flue Gas", *Journal of Hazardous Materials*, Vol.146, pp.1–11.

Yenisoy-Karakaş S., A. Aygün, M. Günes, E. Tahtasakal, 2004, "Physical and Chemical Characteristics of Polymer-Based Spherical Activated Carbon and Its Ability to Adsorb Organics", *Carbon*, Vol. 42, pp.477–484.

Zhuang Q-L., T. Kyotany, A. Tomita, 1994, "The Change of TPD Pattern of O_2-Gasified Carbon Upon Air Exposure", *Carbon*, Vol. 32, pp.539-540.

Zhuang Q-L., T. Kyotany, A. Tomita, 1994, "DRIFT and TK/TPD Analyses of Surface Oxygen Complexes Formed during Carbon Gasification", *Energy and Fuels*, Vol. 8, pp. 714-718.

Zielke U., K. J. Huttinger, W. P. Hoffman, 1996, "Surface-Oxidized Carbon Fibers: I. Surface Structure and Chemistry", *Carbon*, Vol. 34, pp. 983-996.